ORIGINAL RESEARCH

Effect of Active Cancer on the Cardiac Phenotype: A Cardiac Magnetic Resonance Imaging-Based Study of Myocardial Tissue Health and Deformation in Patients With Chemotherapy-Naïve Cancer

Dina Labib [iD], MD; Alessandro Satriano [iD], PhD; Steven Dykstra, MSc; Reis Hansen, BSc; Yoko Mikami [iD], MD, PhD; David G. Guzzardi, PhD; Zdenka Slavikova, BSc; Patricia Feuchter, MSc; Jacqueline Flewitt, MSc; Sandra Rivest, RN; Rosa Sandonato, BScN, RN; Carmen P. Lydell, MD; Andrew G. Howarth, MD, PhD; Louis Kolman, MD; Brian Clarke, MD; D. Ian Paterson [iD], MD; Gavin Y. Oudit [iD], MD, PhD; Edith Pituskin [iD], RN, PhD; Winson Y. Cheung, MD, MPH; Joon Lee [iD], PhD; James A. White [iD], MD

BACKGROUND: The overlap between cancer and cardiovascular care continues to expand, with intersections emerging before, during, and following cancer therapies. To date, emphasis has been placed on how cancer therapeutics influence downstream cardiac health. However, whether active malignancy itself influences chamber volumes, function, or overall myocardial tissue health remains uncertain. We sought to perform a comprehensive cardiovascular magnetic resonance-based evaluation of cardiac health in patients with chemotherapy-naïve cancer with comparison with a healthy volunteer population.

METHODS AND RESULTS: Three-hundred and eighty-one patients with active breast cancer or lymphoma before cardiotoxic chemotherapy exposure were recruited in addition to 102 healthy volunteers. Both cohorts underwent standardized cardiovascular magnetic resonance imaging with quantification of chamber volumes, ejection fraction, and native myocardial T1. Left ventricular mechanics were incrementally assessed using three-dimensional myocardial deformation analysis, providing global longitudinal, circumferential, radial, and principal peak-systolic strain amplitude and systolic strain rate. The mean age of patients with cancer was 53.8±13.4 years; 79% being women. Despite similar left ventricular ejection fraction, patients with cancer showed smaller chambers, increased strain amplitude, and systolic strain rate in both conventional and principal directions, and elevated native T1 versus sex-matched healthy volunteers. Adjusting for age, sex, hypertension, and diabetes mellitus, the presence of cancer remained associated with these cardiovascular magnetic resonance parameters.

CONCLUSIONS: The presence of cancer is independently associated with alterations in cardiac chamber size, function, and objective markers of tissue health. Dedicated research is warranted to elucidate pathophysiologic mechanisms underlying these findings and to explore their relevance to the management of patients with cancer referred for cardiotoxic therapies.

Key Words: cardiac magnetic resonance imaging ■ cardio-oncology ■ chemotherapy-naïve ■ myocardial strain ■ T1 mapping

See Editorial by Chen and Ghosh

CLINICAL PERSPECTIVE

What Is New?

- To date, emphasis has been placed on how cancer therapeutics influence downstream cardiac health. Whether active malignancy itself influences chamber volumes, function, or overall myocardial tissue health remains uncertain.
- Using multi-component cardiovascular magnetic resonance of 381 patients with recently diagnosed breast cancer or lymphoma, we demonstrated unique distributions for a range of imaging markers, inclusive of reduced chamber volumes and elevated strain and native myocardial T1, compared with sex-matched healthy volunteers; these associations remained significant following comprehensive adjustment inclusive of age and cardiovascular risk factors.
- This is the largest and most comprehensive study of cardiovascular phenotype in patients with active (chemotherapy-naïve) cancer.

What Are the Clinical Implications?

- Our results confirm objective and measurable influences of active cancer on the cardiovascular system.
- This discovery is of broad relevance to the practices of cardiology and oncology, and frames future studies aimed at exploring postulated signaling pathways and their downstream influence on subsequent cancer therapeutics-related cardiac dysfunction and cancer-related outcomes.
- Additional consideration should be given to studying influences of de novo cancer development in patients with established cardiovascular disease, justified by its demonstrated potential to alter hemodynamic, contractile, and myocardial tissue level characteristics.

Nonstandard Abbreviations and Acronyms

3D-MDA	three-dimensional myocardial deformation analysis
AHA	American Heart Association
GLS	global longitudinal strain
HV	healthy volunteers
maxPS	maximum principal strain
SSR	systolic strain rate

Expanding intersections between cancer and cardiovascular disease have become increasingly relevant to contemporary clinical practice.[1] In this context, strong emphasis has been placed on how cancer therapeutics may adversely influence downstream cardiovascular health.[2–5] However, several studies have shown strong and independent associations between oncogenesis and heart disease itself,[6–9] supporting that these unique disease states may interact through shared signaling pathways independent of those triggered by cancer therapeutics.[10–12] Preclinical animal studies have offered support for such interactions, demonstrating both structural and innervation-related changes of cardiomyocytes in the setting of active cancer.[13,14] From these studies, the existence of meaningful influences of cancer on the cardiovascular system has been postulated, raising important considerations surrounding how malignancy itself influences cardiovascular health.

To date, the cardiovascular phenotype of patients with newly diagnosed cancer has nominally been considered similar to that of a healthy population. Indeed, this assumption underpins the current population-based lower limit of normal thresholds for defining the occurrence of cancer therapeutics-related cardiac dysfunction (CTRCD).[15,16] However, an understanding of how the presence of malignancy innately influences heart chamber volumes, mass, contractility, and overall myocardial tissue health is uncertain. A reference standard technique for the study of these features is cardiovascular magnetic resonance (CMR), an imaging modality providing unique versatility and accuracy in quantifying cardiac architecture, deformation, and tissue characteristics.

In this prospective cohort study, we used multi-component CMR to examine the cardiac phenotype of patients with recently diagnosed breast cancer or lymphoma, before chemotherapy exposure. These subjects were systematically compared with recruited healthy volunteers (HV) with no history of cancer. Sex-matched comparisons of quantitative markers were performed, inclusive of chamber volumes, left ventricular (LV) mass, bi-ventricular ejection fraction, three-dimensional (3D) strain analysis, and native myocardial T1.

METHODS

The data that support the findings of this study are available from the corresponding author upon reasonable request.

Study Population

Patients were enrolled as part of CAPRI (Cardiotoxicity Prevention Research Initiative), a pre-defined and independently funded sub-study of CIROC (Cardiovascular Imaging Registry of Calgary) (NCT04367220). Enrollment was conducted between January 2015 and December 2019. At time of analysis, CAPRI had prospectively recruited 595

unique patients with cancer referred for CMR imaging. For this analysis, only patients with breast cancer or lymphoma undergoing imaging before receipt of any anthracyclines and/or trastuzumab therapy were considered eligible. Patients with known prior cardiovascular disease or conditions anticipated to confound cardiac phenotype were excluded, inclusive of: known ischemic or non-ischemic cardiomyopathy, LV dysfunction (LV ejection fraction [EF] <50% or regional wall motion abnormality), severe valvular disease (stenosis or regurgitation), moderate/severe pulmonary hypertension, or documented extension of mediastinal cancer distorting cardiac anatomy (as determined by CMR). The final cohort included 381 patients (246 breast cancer and 135 lymphoma).

One hundred two HV were prospectively recruited to establish healthy reference values for all investigated markers of cardiac phenotype. HV were recruited from the local community and were required to have no history of cancer, cardiovascular disease, moderate or severe obesity (body mass index ≥35 kg/m^2), history of hypertension, diabetes mellitus, kidney, or collagen vascular disease.

The study was approved by the Conjoint Health Research Ethics Board at the University of Calgary (REB 13-0902) and all subjects provided written informed consent. All research activities were performed in accordance with the Declaration of Helsinki.

Cardiovascular Risk Factors

All subjects underwent baseline surveys of comorbid health and cardiovascular risk factors, with abstraction of all clinically performed laboratory testing. Subjects were coded as hypertensive if receiving anti-hypertensive medications for known hypertension or had ≥3 blood pressure readings ≥140/90 mm Hg within 12 months before CMR imaging. Diabetes mellitus was coded as present if receiving oral hypoglycemics or insulin or had a Hemoglobin A1c ≥6.5% within 3 years before or 4 months following index CMR. Dyslipidemia was coded as follows: treated if receiving lipid-lowering therapy and untreated for a low-density lipoprotein cholesterol ≥3.5 mmol/L or triglycerides ≥1.7 mmol/L documented within 3 years before or 4 months following index CMR.

CMR Imaging Protocol

Subjects were scanned using 1.5-T (Avanto; 34 patients with cancer) or 3.0-T (Prisma or Skyra; 347 patients with cancer, all HV) systems (Siemens Healthcare, Erlangen, Germany). All underwent standardized, non-contrast imaging protocols inclusive of routine cine imaging and native T1 mapping. Cine imaging was performed in sequential short axis (8-mm thickness; 2-mm gap) and conventional long-axis views (4-chamber, 2-chamber, and 3-chamber) at end-expiration using a steady-state free precession pulse sequence. Native T1 mapping was performed in short axis at the mid-LV level using a Shortened Modified Look-Locker Inversion Recovery sequence, as previously described.[17]

Quantification of Cardiac Chamber Volumes and LV Mass

Quantification of LV, right ventricular (RV), and left atrial (LA) volumes was performed using commercially available software (cvi**42**; Circle Cardiovascular Imaging Inc., Calgary, Canada) and standard operational procedures adherent to the published Society of Cardiovascular Magnetic Resonance recommendations.[18] Semi-automated tracing of endocardial and epicardial contours of short-axis cine images was used to derive the LV and RV end-diastolic volumes, end-systolic volumes, and ejection fraction, as well as LV mass. Papillary muscles were included in the LV mass and excluded from LV cavitary volume. LA volume was measured at the LV end-systolic phase before mitral valve opening using the bi-plane area-length method from temporally matched 4- and 2-chamber cine views. Volumetric indices and LV mass were indexed both to body surface area (BSA; Mosteller formula) and to height, the latter to mitigate confounding effects related to cancer-mediated cachexia.

Global and Regional Myocardial Deformation Analysis

Three-dimensional myocardial deformation analysis (3D-MDA) was performed using validated in-house software for the global and regional description of conventional geometry-dependent (radial, circumferential, and longitudinal) and geometry-independent (maximal and minimal principal) strain. As previously described,[19,20] this approach generates a 3D mesh model of the LV following automated registration and alignment of short- and long-axis 2-dimensional (2D) cine data sets, accounting for inter-slice respiratory motion. The resultant model is deformed using a virtual 4-dimensional displacement field obtained from all available voxel data. Deformation variables were provided in both global and segmental measures, the latter provided according to the American Heart Association (AHA) 17-segmental model,[21] excluding the apical cap. In addition to longitudinal, circumferential, and radial strain profiles, we incrementally calculated principal strain to provide an unbiased description of deformation, inclusive of shear deformation.[22] All measures were provided as peak systolic strain amplitude and peak systolic strain rate (SSR).

As 3D strain amplitudes are recognized to be unique (ie, lower) versus 2D strain measures,[23] all comparisons were made to identical 3D-MDA analyses performed in sex-matched HV.

Native T1 Mapping Analysis

For patients imaged at 3.0-T, native T1 was measured by region of interests applied to the LV septum (AHA segments 8 and 9) and lateral wall (AHA segments 11 and 12) on the mid-ventricular slice. Region of interests were restricted to the mid-myocardium to avoid partial volume effects and all raw images were assessed to account for respiratory drift or gating-related image misregistration. Artefacts, when present, were manually excluded.

Statistical Analysis

Continuous variables were expressed as mean±SD or median (interquartile range); categorical variables as counts (percentage). Two-group comparisons (patients with cancer versus HV) were performed using 2-sample t-test/Mann-Whitney test for continuous variables, or Chi-square/Fisher exact test for categorical variables where appropriate. For 3-group comparisons (breast cancer/lymphoma/HV and cancer with/without cardiovascular risk factors/HV), 1-way Welch ANOVA or Kruskal–Wallis test were used, with post-hoc pairwise comparisons performed using Games–Howell test for the former and Dunn procedure with Bonferroni correction for the latter.

Multiple linear regression was used to test for association between the presence of cancer (as predictor) and each of the investigated CMR variables (such as LV end-diastolic volumes or strain amplitude; as an outcome), adjusting for age, sex, hypertension, and diabetes mellitus.

Statistical analyses were conducted using R version 3.6.2 and SPSS version 26, with 2-tailed $P<0.05$ indicating statistical significance. Bull's eye plots of American Heart Association (AHA) 17-segment model for regional distribution of myocardial strain were produced using Python package Matplotlib version 3.1.3.

RESULTS

Clinical Characteristics of Study Cohort

The study population consisted of 381 patients with chemotherapy-naïve cancer and 102 HV. Baseline clinical characteristics of patients are shown in Table 1. The majority (n=246; 65%) had breast cancer with the remainder having lymphoma (n=135; 35%). The majority were female (n=300; 79%) with a

Table 1. Baseline Clinical Characteristics of Study Patients (n=381)

Characteristic	Descriptive Statistics
Age, y	53.8±13.4
Female sex	300 (79%)
Cigarette smoking	
Never	307 (81%)
Current	40 (11%)
Former	34 (9%)
Alcohol intake	
None	106 (28%)
Occasional (<1 drink/d)	214 (56%)
Moderate (1–2/d)	49 (13%)
Heavy (>2/d)	9 (2%)
QoL (rating on 0–100 scale)*	75.0 (60.0–90.0)
Hypertension	129 (34%)
Diabetes mellitus	40 (11%)
Dyslipidemia	175 (46%)
Treated	58 (15%)
Untreated	117 (31%)
History of CAD	7 (2%)
History of CAD-equivalent (cerebrovascular, PVD)	11 (3%)
Known kidney disease†	16 (4%)
Collagen vascular disease	11 (3%)
BMI, kg/m²	26.6 (23.3–30.9)
BMI status	
Underweight (BMI <18.5 kg/m²)	4 (1%)
Normal weight (BMI 18.5–24.9 kg/m²)	142 (38%)
Overweight (BMI 25–29.9 kg/m²)	124 (33%)
Mild/moderate obesity (BMI 30–39.9 kg/m²)	89 (24%)
Morbid obesity (BMI ≥40 kg/m²)	17 (5%)
Baseline atrial fibrillation/flutter	4 (1%)
Laboratory tests	
Hemoglobin, g/L	136.0 (127.0–143.0)
GFR, mL/min	96.1 (74.5–118.2)
Medications	
Aspirin	25 (7%)
Beta-blocker	26 (7%)
ACEi/ARB	81 (21%)
Calcium channel blocker	31 (8%)
Statin	55 (14%)
Cancer characteristics	
Cancer type	
Breast cancer	246 (65%)
HER2 receptor	
Negative	114 (46%)
Positive	128 (52%)
Equivocal	4 (1%)
Estrogen receptor positive	185 (75%)

(Continued)

Table 1.   Continued

Characteristic	Descriptive Statistics
Progesterone receptor positive	142 (58%)
Lymphoma	135 (35%)
Tumor AJCC stage	
I	104 (27%)
II	133 (35%)
III	68 (18%)
IV	75 (20%)
Duration since diagnosis, mo	1.2 (0.8, 2.5)
Prior cancer‡	34 (9%)
Prior radiotherapy to breast/mediastinum	6 (2%)

Values are mean±SD, median (IQR), or n (%). ACEi indicates angiotensin converting enzyme inhibitor; AJCC, American Joint Committee on Cancer; ARB, angiotensin receptor blocker; BMI, body mass index; CAD, coronary artery disease; GFR, glomerular filtration rate; HER2, human epidermal growth factor receptor-2; PVD, peripheral vascular disease; and QoL, quality of life.

*Available for 280 patients.

†Defined as abnormalities of kidney function or structure present for >3 months, including GFR <60 mL/min, urinary albumin/creatinine ratio >3 mg/mmol, history of renal transplantation, or solitary kidney.

‡Not treated with anthracycline or trastuzumab.

mean age 53.8±13.4 years (range, 22.3–89.2 years). The HV cohort included 55 women (54%); mean age, 43.4±14.5 years (range, 19.0–80.0 years). The mean body mass index of this reference cohort was 25.2±3.7 kg/m². In accordance with strict recruitment criteria, no HV had any cardiovascular disease, was receiving medication for a cardiovascular or cancer diagnosis, or had any other comorbidity listed in Table 1.

Patients with cancer showed an expected prevalence of conventional cardiovascular risk factors (Table 1). Hypertension, diabetes mellitus, dyslipidemia, and current cigarette smoking were present in 34%, 11%, 46%, and 11% of patients; respectively. Approximately one-fifth were receiving angiotensin-converting enzyme inhibitors and 14% statin therapy. Sixty-two percent were overweight or obese, only 1% being underweight.

As shown in Tables 2 and 3, patients with cancer showed higher heart rates (mean increase 6.8 bpm in women and 11.2 bpm in men), with similar systolic and diastolic blood pressures versus HV. Female, but not male, patients with cancer had higher body mass index compared with HV (median increase, 2.4 and 0.7 kg/m², respectively).

CMR Phenotypic Characteristics of Patients With Cancer

As shown in Tables 2 and 3, numerous CMR phenotypic characteristics were found to be altered in patients with cancer versus HV.

Cardiac Chamber Volumes and LV Mass

Compared with HV, patients with cancer had similar LV EF but statistically significant elevation in RV EF (mean absolute difference of 1.9% in women and 3.2% in men). Patients with cancer had significantly smaller LV, RV, and LA volumes compared with HV. In women with cancer, BSA-indexed LV end-diastolic volumes, RV end-diastolic volumes, and LA volume were 13% lower. In men with cancer, respective reductions were 12%, 15%, and 11%. These led to significant reductions in stroke volume, these appropriately compensated for by higher heart rates to achieve similar cardiac output to HV. Female, but not male, patients with cancer showed higher LV mass (increase of 7%). Findings were similar after exclusion of those patients with cancer scanned at 1.5-T (n=34).

Repeat indexing of chamber volumes and LV mass to height alone yielded similar results, the exception being LA volumes were no longer significantly different among men (Table S1).

Global and Regional Myocardial Deformation

Three-dimensional-MDA analysis was feasible in 357 patients with cancer and 100 HV following the exclusion of studies with insufficient image quality. For simplicity, only transmural strain values are described, with subendocardial and subepicardial layer strain values provided in Table S2.

As shown in Tables 2, 3, and Figure 1, geometry-dependent and principal global peak systolic strain amplitudes and SSR were elevated in both female and male patients with cancer versus HV. The only observed exception was global longitudinal strain (GLS) amplitude in women, which was not significantly different. Maximal principal strain (maxPS) and radial strain showed the greatest elevation in global peak systolic amplitude and SSR, with a relative increase that exceeded 10% versus HV. Findings were similar after exclusion of those patients with cancer scanned at 1.5-T (n=34). Results for layer-specific strain were similar except for a few markers not reaching statistical significance (Table S2).

Regional alterations in myocardial mechanics were explored by segmental analysis. Here, focus was placed on maxPS as an un-biased, geometry-independent, and comprehensive measure of local tissue deformation. Figures 2 and 3 display bullseye plots for this marker to illustrate differences in median maxPS amplitude and SSR in patients with cancer versus HV, stratified by sex, for each of the AHA 16 segments. Significant (P<0.05) differences were observed by segmental pairwise comparisons for both sex cohorts, as indicated by asterisks. Non-uniformity of myocardial deformation measures in

Table 2. Baseline CMR Characteristics of Female Patients With Chemotherapy-Naïve Cancer Compared With Healthy Volunteers

Characteristic	Healthy Volunteers (n=55)	Patients With Cancer (n=300)	*P* Value
Age, y	41.9±13.8	52.5±12.7	<0.001
BMI, kg/m²	24.1 (21.0–27.7)	26.5 (22.9–30.8)	<0.001
Heart rate, bpm	64.7±10.3	71.5±11.7	<0.001
Systolic BP, mm Hg	110.9±12.5	116.7±15.7	0.004
Diastolic BP, mm Hg	65.8±9.2	69.1±11.3	0.023
CMR characteristics			
Chamber volumes and mass (indexed to BSA)			
LV EDV, mL/m²	77.9±12.0	68.1±11.8	<0.001
LV ESV, mL/m²	27.6±6.4	23.9±6.4	<0.001
LV EF, %	64.8±5.0	65.1±5.5	0.65
LV mass, g/m²	41.3±6.6	44.2±8.4	0.006
LV stroke volume, mL/m²	50.3±7.8	44.1±7.3	<0.001
LV cardiac output, mL/m² per min	3.3±0.6	3.1±0.6	0.18
RV EDV, mL/m²	83.1±12.7	69.3±12.6	<0.001
RV ESV, mL/m²	34.3±7.8	27.3±7.2	<0.001
RV EF, %	59.0±5.0	60.9±6.1	0.013
RV stroke volume, mL/m²	48.8±7.0	42.0±7.8	<0.001
RV cardiac output, mL/m² per min	3.2±0.6	3.0±0.6	0.022
LA volume, mL/m²	34.7±6.0	30.2±8.1	<0.001
3D-MDA*			
Circumferential strain amplitude, %	−11.1±1.8	−11.8±1.8	0.008
Longitudinal strain amplitude, %	−11.6±1.7	−11.9±1.9	0.28
Radial strain amplitude, %	64.3±19.1	71.7±26.3	0.015
Minimum principal strain amplitude, %	−27.0±2.3	−28.7±2.6	<0.001
Maximum principal strain amplitude (%)	88.8 (79.3–95.8)	102.4 (84.9–125.0)	<0.001
Systolic circumferential strain rate (1/s)	−0.88±0.15	−0.93±0.15	0.037
Systolic longitudinal strain rate (1/s)	−1.05±0.16	−1.13±0.21	0.002
Systolic radial strain rate (1/s)	4.38 (3.90–5.21)	5.19 (4.06–6.52)	0.003
Systolic minimum principal strain rate (1/s)	−1.75±0.35	−1.87±0.34	0.018
Systolic maximum principal strain rate (1/s)	5.50 (4.67–6.25)	6.41 (5.13–8.09)	<0.001
Native T1			
Septum, ms†	1143.5 (1121.3–1161.0)	1166.5 (1142.0–1190.3)	<0.001
Lateral wall, ms‡	1130.0 (1096.3–1165.8)	1149.0 (1120.0–1183.0)	0.020

Values are mean±SD, median (IQR), or n (%). 3D-MDA indicates three-dimensional myocardial deformation analysis; BMI, body mass index; BP, blood pressure; BSA, body surface area; CMR, cardiovascular magnetic resonance; EDV, end-diastolic volume; EF, ejection fraction; ESV, end-systolic volume; LA, left atrium; LV, left ventricle; and RV, right ventricle.

*Global values; available for 285 patients with cancer and 55 healthy volunteers.

†Available for 238 patients with cancer and 38 healthy volunteers imaged at 3.0-T.

‡Available for 225 patients with cancer and 36 healthy volunteers imaged at 3.0-T.

healthy individuals was confirmed, with characteristically higher strain values for apical segments and relatively lower values for basal septal segments. Patients with cancer demonstrated exaggeration of this normally observed pattern of deformation, with significant elevations observed in maxPS amplitude for multiple segments (Figure 2). For example, median maxPS amplitude showed an absolute 36.6% increase for the apical septal segment in female patients with cancer (178.9% versus 142.3%, *P*=0.002) and 31.1% increase in men (154.5%

versus 123.4%, *P*=0.02) versus HV. Similar findings were observed for maxPS SSR (Figure 3). Identical analyses performed for the measures of longitudinal, circumferential, radial, and minimum principal strain showed similar geographic exaggerations in strain amplitude and SSR.

Native T1 Mapping

Native T1 mapping analysis was successfully completed for 299 patients with cancer and 77 HV

Table 3. Baseline CMR Characteristics of Male Patients With Chemotherapy-Naïve Cancer Compared With Healthy Volunteers

Characteristic	Healthy Volunteers (n=47)	Patients with Cancer (n=81)	*P* Value
Age, y	45.1±15.3	58.8±14.6	<0.001
BMI, kg/m^2	26.2 (24.3–29.1)	26.9 (24.5–31.1)	0.21
Heart rate, bpm	61.3±9.3	72.5±12.9	<0.001
Systolic BP, mm Hg	115.2±11.8	119.7±19.9	0.12
Diastolic BP, mm Hg	67.7±11.0	71.6±10.8	0.066
CMR characteristics			
Chamber volumes and mass (indexed to BSA)			
LV EDV, mL/m^2	84.9±11.8	74.6±14.8	<0.001
LV ESV, mL/m^2	31.6±5.9	27.0±7.4	<0.001
LV EF, %	62.9±3.7	64.0±5.9	0.22
LV mass, g/m^2	57.2±11.8	54.6±12.6	0.25
LV stroke volume, mL/m^2	53.3±7.3	47.6±9.7	<0.001
LV cardiac output, mL/m^2 per min	3.2±0.5	3.4±0.8	0.12
RV EDV, mL/m^2	96.1±12.9	79.7±17.1	<0.001
RV ESV, mL/m^2	42.8±7.9	33.1±9.8	<0.001
RV EF, %	55.6±4.4	58.8±5.8	<0.001
RV stroke volume, mL/m^2	53.3±7.6	46.6±9.7	<0.001
RV cardiac output, mL/m^2 per min	3.3±0.5	3.3±0.8	0.41
LA volume, mL/m^2	35.7±8.3	31.8±10.4	0.024
3D-MDA*			
Circumferential strain amplitude, %	−10.7±1.7	−11.7±2.4	0.012
Longitudinal strain amplitude, %	−10.6±1.4	−11.7±2.3	0.003
Radial strain amplitude, %	50.8±20.0	63.1±23.0	0.003
Minimum principal strain amplitude, %	−24.9±2.9	−26.9±3.2	<0.001
Maximum principal strain amplitude (%)	67.5 (57.8–86.2)	86.9 (69.8–103.8)	0.002
Systolic circumferential strain rate (1/s)	−0.84±0.17	−0.98±0.17	<0.001
Systolic longitudinal strain rate (1/s)	−0.97±0.17	−1.16±0.21	<0.001
Systolic radial strain rate (1/s)	3.70 (2.96–4.42)	4.78 (3.85–6.29)	<0.001
Systolic minimum principal strain rate (1/s)	−1.66±0.33	−1.89±0.42	0.001
Systolic maximum principal strain rate (1/s)	4.56 (3.50–5.91)	5.65 (4.62–7.61)	<0.001
Native T1			
Septum, ms†	1104.0 (1073.0–1140.0)	1173.0 (1142.0–1210.5)	<0.001
Lateral wall, ms‡	1096.0 (1069.5–1122.5)	1155.0 (1130.0–1193.5)	<0.001

Values are mean±SD, median (IQR), or n (%). 3D-MDA indicates 3-dimensional myocardial deformation analysis; BMI, body mass index; BP, blood pressure; BSA, body surface area; CMR, cardiovascular magnetic resonance; EDV, end-diastolic volume; EF, ejection fraction; ESV, end-systolic volume; LA, left atrium; LV, left ventricle; and RV, right ventricle.

*Global values; available for 72 patients with cancer and 45 healthy volunteers.

†Available for 61 patients with cancer and 39 healthy volunteers imaged at 3.0-T.

‡Available for 53 patients with cancer and 37 healthy volunteers imaged at 3.0-T.

imaged at 3.0-T. The mid-septal segments were analyzable in all subjects, and for 278 patients and 73 HV for the lateral wall segments. As shown in Tables 2 and 3, both female and male patients with cancer showed higher native T1 values versus HV. The median elevation in females was 23 ms in the septum (1167 ms versus 1144 ms, *P*<0.001) and 19 ms in the lateral wall (1149 ms versus 1130 ms, *P*=0.02). The median elevation in men was 69 ms in the septum (1173 ms versus 1104 ms, *P*=0.001) and 59 ms in the lateral wall (1155 ms versus 1096 ms, *P*<0.001).

Multivariable Association of Cancer and CMR markers

To test for independent associations of cancer with each studied CMR parameter adjusting for relevant
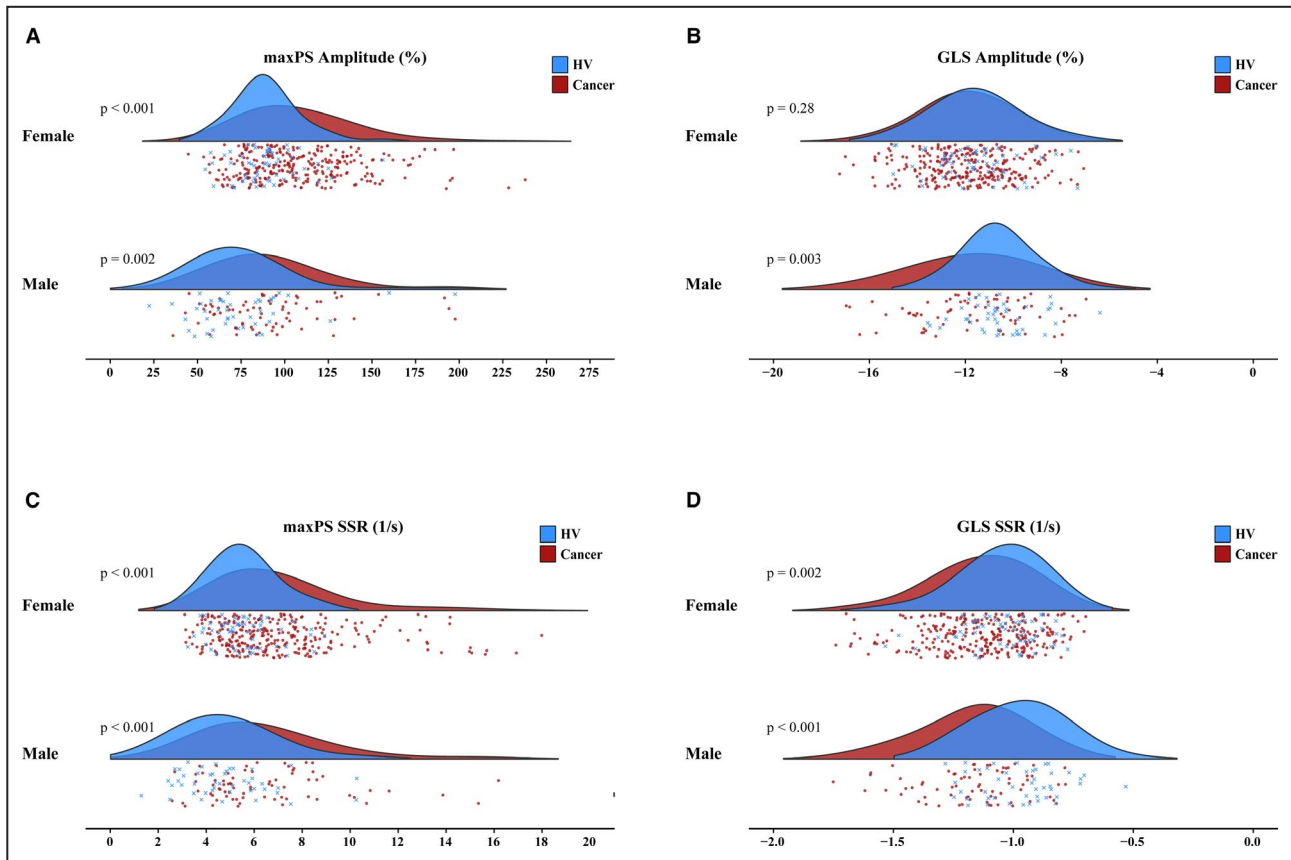
Figure 1. Strain parameters (global maximum principal and longitudinal strain amplitude [A and B] and peak systolic strain rate [SSR; C and D]) in patients with chemotherapy-naïve cancer vs healthy volunteers, stratified by sex.
Absolute values of all parameters, except GLS amplitude, were higher in patients with cancer vs sex-matched healthy volunteers. GLS indicates global longitudinal strain; HV, healthy volunteers; maxPS; maximum principal strain; and SSR, systolic strain rate.

demographics and cardiovascular risk factors, we constructed multivariable models for each parameter as the outcome, adjusting for age, sex, hypertension, and diabetes mellitus. As shown in Table 4, cancer presence remained strongly predictive of global maxPS amplitude (P=0.007) with an adjusted mean absolute elevation of 10% (95% CI, 3%–17%) versus HV. Table 5 shows multivariable associations for cancer presence and all studied CMR variables. Cancer presence remained independently associated with lower chamber volumes, higher strain parameters (with exception of GLS amplitude), and higher native T1 values. Following adjustment, cancer presence was no longer associated with increased LV mass.

Sensitivity Analyses

To confirm independence of the observed phenotypic changes from cancer type and cardiovascular risk factors, we performed targeted sensitivity analyses.

Effect of Cancer Type

A priori sensitivity analysis was performed to assess confounding effects of cancer type. As shown in Figure 4 and Table S3 for female subjects, no significant differences in CMR characteristics were seen between the 2 cancer types. Overall, both cancer types showed similar differences in CMR characteristics versus HV. Patients with breast cancer (n=242), but not lymphoma (n=58), showed higher LV mass. The reduced population sizes resulted in a loss of significance for several 3D-MDA measures; however, similar trends were maintained. Native T1 values of the septum remained significantly elevated in both cancer subtypes compared with HV. Since only 4 male patients had breast cancer, subgroup analysis for male subjects was only performed in patients with lymphoma, demonstrating similar results to the overall male cancer cohort (Table S4).

Effect of Cardiovascular Risk Factors

To explore potential influences of cardiac risk factors on patient phenotype, we assessed associations between
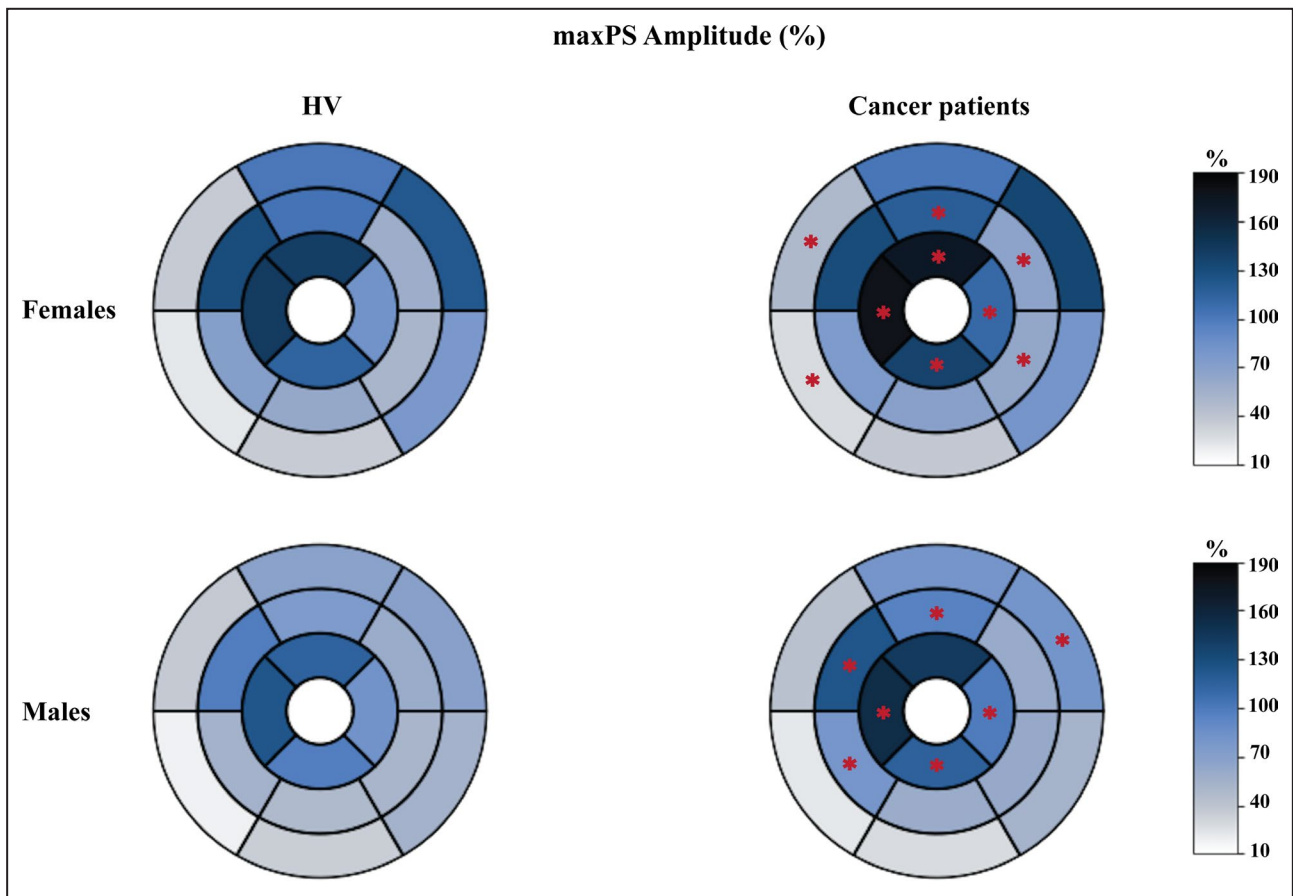
Figure 2.   Bullseye view of 3-dimensional spatial analysis of median regional maximum principal strain amplitude (%) in patients with cancer vs healthy volunteers, stratified by sex.

Asterisks denote segments with *P*<0.05 for comparison of patients with cancer vs sex-matched healthy volunteers. Healthy volunteers showed non-uniformity of myocardial deformation throughout left ventricular segments, with higher strain amplitude in the apical segments and relatively lower values for basal septal segments; healthy volunteers showed amplification of this pattern. HV indicates healthy volunteers; maxPS; maximum principal strain; and SSR, systolic strain rate.

cancer presence and CMR characteristics among subgroups with and without hypertension and diabetes mellitus. These results are summarized in Tables 6, 7, and Figure 5. In patients with cancer with hypertension, an anticipated elevation in LV mass with reduced ventricular volumes was observed versus those without hypertension. The previously observed chamber volumes', strain, and native T1 associations with cancer presence were maintained irrespective of hypertension. In patients with cancer with diabetes mellitus, we observed similar LV mass but smaller biventricular volumes and higher septal native T1 versus those without diabetes mellitus. All chamber volumes', strain and native T1 associations with cancer presence were maintained irrespective of diabetes mellitus, except for GLS and global radial strain amplitude which lost significance among those with diabetes.

Finally, we repeated comparisons of patients with cancer versus sex-matched HV following the exclusion of patients with either diabetes mellitus or hypertension (n=137). Repeat subgroup analyses for female patients

with cancer showed maintained significance for all parameters except LV mass and global circumferential SSR. Repeat subgroup analysis in male patients with cancer was limited by small sample size (n=34). Despite this, maintained statistical significance was observed for native T1, GLS amplitude and SSR, stroke volumes, and RV volumes; the remaining parameters all showing trends in the same direction as the full study population.

DISCUSSION

To our knowledge, this is the largest and most comprehensive study of cardiovascular phenotype in patients with active (chemotherapy-naïve) cancer. Using multicomponent CMR of patients with recently diagnosed breast cancer or lymphoma, we demonstrated unique distributions for a range of markers, inclusive of reduced cardiac chamber volumes, reduced stroke volume, elevated global and regional strain, and elevated native myocardial T1 compared with sex-matched HV.
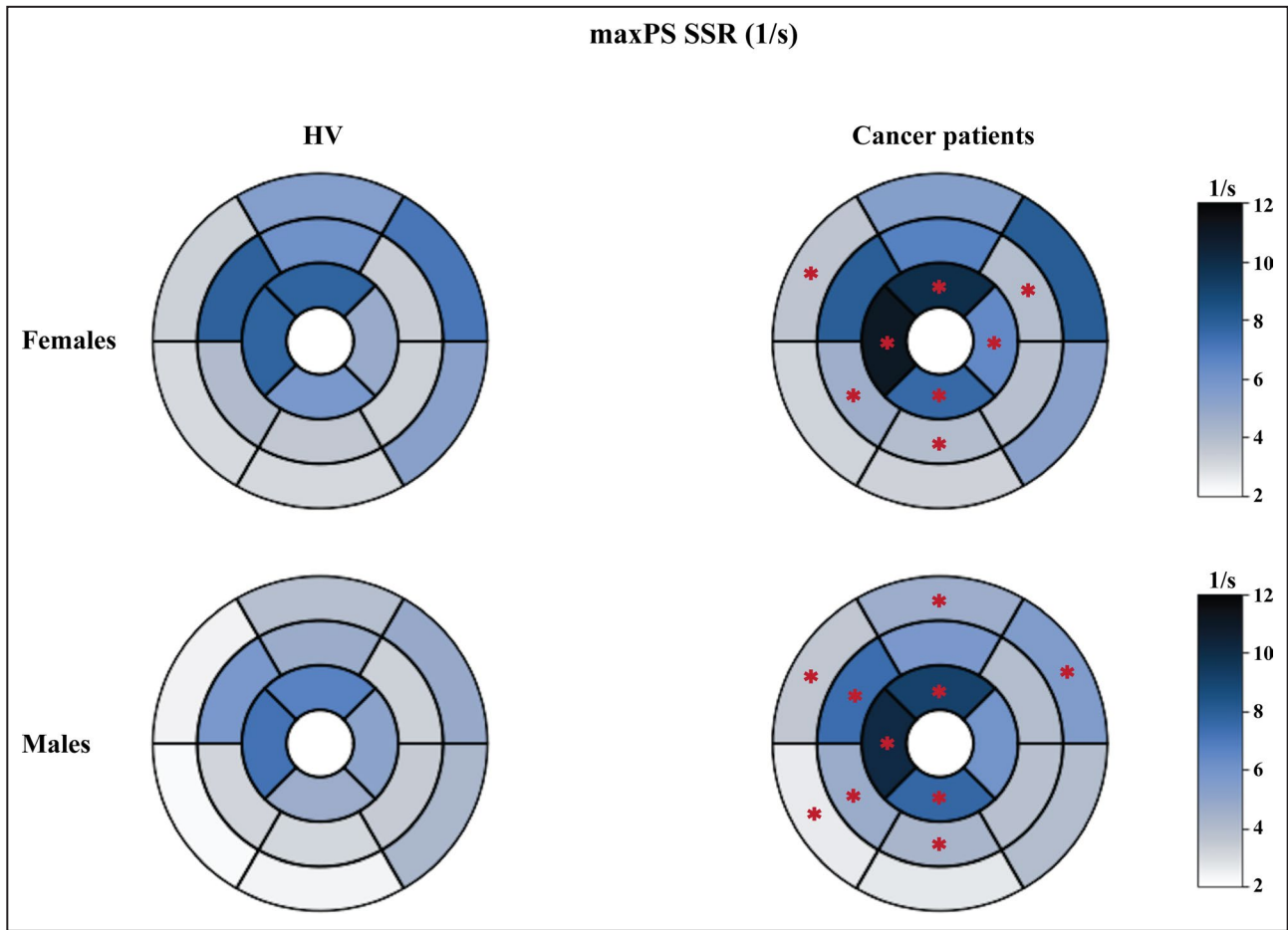
Figure 3.   Bullseye view of 3-dimensional spatial analysis of median regional maximum principal systolic strain rate (1/s) in patients with cancer vs healthy volunteers, stratified by sex.
Asterisks denote segments with $P<0.05$ for comparison of patients with cancer vs sex-matched healthy volunteers. Similar patterns to those in Figure 2 were noted. HV indicates healthy volunteers; maxPS; maximum principal strain; and SSR, systolic strain rate.

These findings were independent of age, hypertension, and diabetes mellitus. A summary of the main findings of our study is provided in Figure 6.

While unified explanations for the observed cancer phenotype will be discussed, independent explanation of the observed architectural, deformation, and tissue-related features is justified.

Cardiac Chamber Remodelling

We observed that patients with cancer have smaller chamber volumes versus sex-matched HV, this consistently observed following indexing to either BSA or height alone. The latter approach was incrementally performed to address potential confounding effects from cancer-related cachexia, this

Table 4.   Results of Multivariable Linear Regression for Association Between Maximum Principal Strain Amplitude and Cancer Presence, Adjusting for Age, Sex, Hypertension, and Diabetes Mellitus

Variable	B*	95% CI for B		P Value for B
		Lower Limit	Upper Limit	
Cancer presence	9.98	2.70	17.25	0.007
Age	0.48	0.27	0.70	<0.001
Female sex	18.68	12.20	25.16	<0.001
Hypertension	6.43	−0.76	13.63	0.079
Diabetes mellitus	−7.46	−18.32	3.40	0.18
Constant	33.10	17.70	48.50	<0.001

*Unstandardized regression coefficient.

Table 5. Results of Multivariable Linear Regression for Association Between Each CMR Variable and Cancer Presence, Adjusting for Age, Sex, Hypertension, and Diabetes Mellitus

CMR Variable	B* for Cancer Presence	95% CI for B		P Value for B
		Lower Limit	Upper Limit	
Chamber volumes and mass (indexed to BSA)				
LV EDV, mL/m²	−6.02	−8.91	−3.12	<0.001
LV ESV, mL/m²	−1.77	−3.30	−0.25	0.023
LV EF, %	−0.68	−1.97	0.61	0.30
LV mass, g/m²	−0.36	−2.67	1.95	0.76
LV stroke volume, mL/m²	−4.24	−6.12	−2.37	<0.001
LV cardiac output, mL/m² per min	0.12	−0.03	0.27	0.11
RV EDV, mL/m²	−9.69	−12.81	−6.58	<0.001
RV ESV, mL/m²	−5.14	−6.96	−3.32	<0.001
RVEF, %	1.26	−0.15	2.66	0.080
RV stroke volume, mL/m²	−4.56	−6.47	−2.64	<0.001
RV cardiac output, mL/m² per min	0.07	−0.08	0.22	0.38
LA volume, mL/m²	−4.40	−6.47	−2.34	<0.001
3D-MDA†				
Circumferential strain amplitude, %	−0.53	−1.00	−0.06	0.027
Longitudinal strain amplitude, %	0.47	−0.01	0.94	0.053
Radial strain amplitude, %	6.35	0.27	12.42	0.041
Minimum principal strain amplitude, %	−1.31	−1.98	−0.64	<0.001
Maximum principal strain amplitude, %	9.98	2.70	17.25	0.007
Systolic circumferential strain rate (1/s)	−0.07	−0.11	−0.03	<0.001
Systolic longitudinal strain rate (1/s)	−0.11	−0.16	−0.06	<0.001
Systolic radial strain rate (1/s)	0.77	0.31	1.24	0.001
Systolic minimum principal strain rate (1/s)	−0.16	−0.25	−0.07	0.001
Systolic maximum principal strain rate (1/s)	0.91	0.31	1.51	0.003
Native T1				
Septum, ms‡	46.26	33.96	58.56	<0.001
Lateral wall, ms§	41.29	27.29	55.30	<0.001

3D-MDA indicates three-dimensional myocardial deformation analysis; BSA, body surface area; CMR, cardiovascular magnetic resonance; EDV, end-diastolic volume; EF, ejection fraction; ESV, end-systolic volume; LA, left atrium; LV, left ventricle; and RV, right ventricle.

*Unstandardized regression coefficient for association between cardiovascular magnetic resonance variable and cancer presence, adjusting for age, sex, hypertension, and diabetes mellitus.

†Global values; available for 457 subjects (357 patients with cancer and 100 healthy volunteers).

‡Available for 376 subjects (299 patients with cancer and 77 healthy volunteers) imaged at 3.0-T.

§Available for 351 subjects (278 patients with cancer and 73 healthy volunteers) imaged at 3.0-T.

disproportionally reducing BSA, and recognized to be accompanied by cardiac muscle atrophy.[24] That no differences were observed by the indexing technique is reflective of a lack of significant weight loss appreciated in the study cohort. This is explained by the recent timing of cancer diagnosis (median time from diagnosis 1.2 months), allowing for less confounding effects of cancer-related cachexia on our study findings. All cardiac chambers' volumes were reduced by a similar proportion without a significant reduction in LV mass, supporting the presence of globally reduced loading conditions. Lower resultant stroke volumes were compensated for by higher resting heart rates.

To date, 3 prior CMR-based studies have been performed in patients with chemotherapy-naïve cancer. Two studies indirectly reported data on LV volumes and mass versus cancer-free controls; however, statistical group comparisons were not performed.[2,25] LV volumes, stroke volume, and LV EF appeared similar in these small studies. A third, recently reported study focused on comparison of LV mass between 28 patients with chemotherapy-naïve breast cancer and 17 age-matched healthy females.[12] This was accompanied by an exploratory in-vitro experiment exposing cultured human cardiomyocytes to a conditioned medium of human breast cancer cells known to be rich in cancer secreting
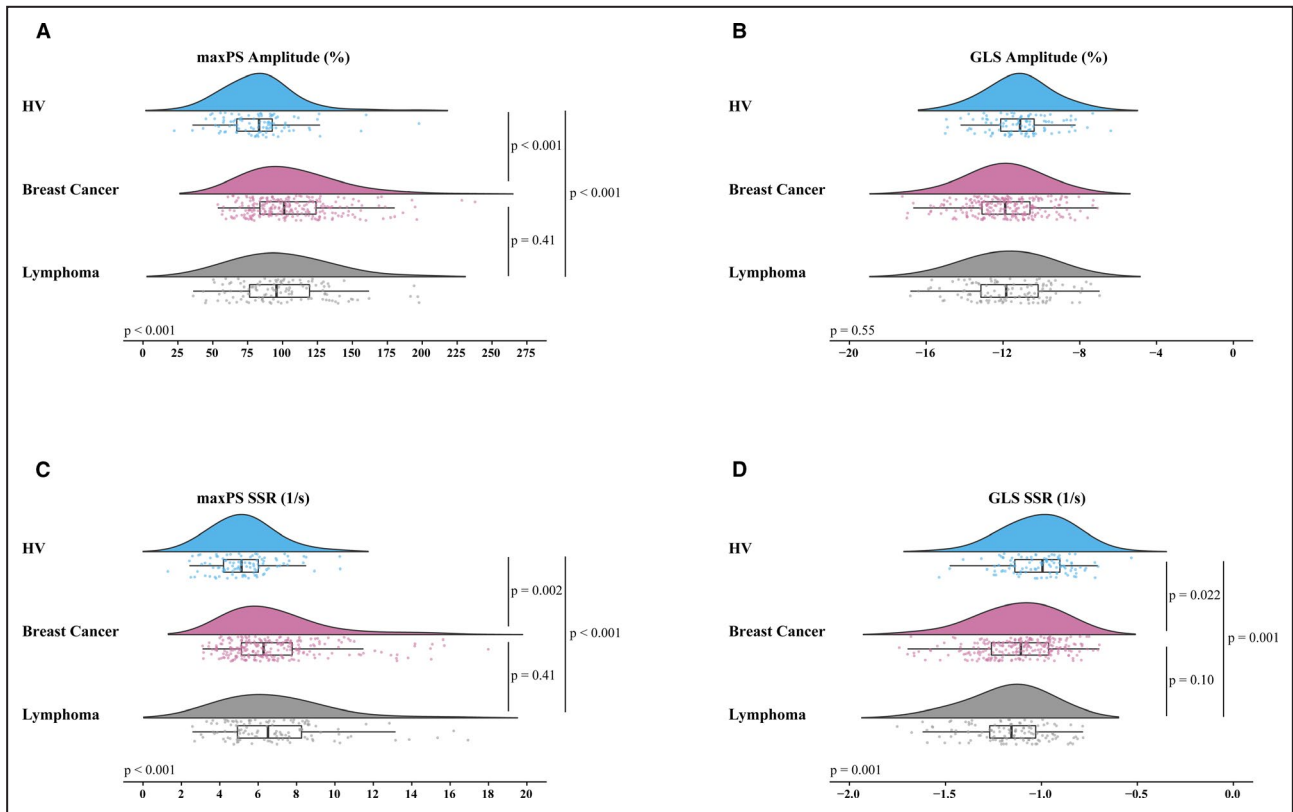
Figure 4. Effect of cancer type on global maximum principal and global longitudinal strain amplitude (A and B) and peak systolic strain rate (C and D) in female patients with cancer vs healthy volunteers.
Absolute values of all parameters were similar in breast cancer and lymphoma subtypes; all except global longitudinal strain amplitude, were higher in each cancer subgroup vs healthy volunteers. GLS indicates global longitudinal strain; HV, healthy volunteers; maxPS; maximum principal strain; and SSR, systolic strain rate.

factors. In this study, a higher LV mass was observed in patients with breast cancer, this postulated to be related to tumor-derived endothelin-1. We confirm this elevation in LV mass among our patients with breast cancer.

Several studies using 2D echocardiographic techniques have been performed in both adult[26–29] and pediatric[30,31] populations with chemotherapy naïve cancer but have yielded conflicting results on LV volumes and mass, largely because of heterogeneous durations of cancer, broad collections of cancer types,[26,27,31] or cancer types different to breast cancer or lymphoma.[28–30] In contrast, our study focused on patients with breast cancer and lymphoma, a population selected for their high referral rate for cardiotoxic therapeutic regimens.

Myocardial Deformation

Patients with cancer demonstrated higher global strain amplitudes and SSR compared with HV, being observed for both geometry-dependent and principal directions of deformation. Segmental analyses identified generalized amplification of the normally encountered geographic pattern of deformation.

Only 1 prior study has directly evaluated myocardial strain profiles of patients with chemotherapy-naïve cancer, in this case matched to patients without cancer from a local clinical service.[26] This was a retrospective study of 122 patients with mixed cancer referred for 2D speckle-tracking echocardiography. The population predominantly had gastrointestinal cancers with some gynecologic, breast and lung cancers, as well as sarcoma, and the duration of cancer was not reported. GLS and global circumferential strain amplitude were found to be lower compared with 45 patients without cancer. However, given the heterogeneity of the population, unknown duration of disease, and lack of a healthy control group, it is challenging to compare this study's results to our own.

It is important to acknowledge technique-specific dependencies of strain evaluations, particularly relevant to 3D versus 2D techniques. In the current study, we used custom, in-house software[19,20] to provide comprehensive 3D evaluations

Table 6. Baseline Characteristics of Patients With Chemotherapy-Naïve Cancer, Stratified by Hypertension, Compared With Healthy Volunteers

Characteristic	Healthy Volunteers (n=102)	Cancer, No Hypertension (n=252)	Cancer, Hypertension (n=129)	P Value
Age, y	43.4±14.5	50.2±13.0*	60.8±11.2*,†	<0.001
BMI, kg/m²	24.9 (22.0–28.4)	25.7 (22.5–29.1)	27.6 (24.6–33.0)*,†	<0.001
Heart rate, bpm	63.1±9.9	70.7±10.9*	73.6±13.5*	<0.001
Systolic BP, mm Hg	112.8±12.3	112.2±12.9	127.5±18.6*,†	<0.001
Diastolic BP, mm Hg	66.6±10.0	67.2±10.0	74.5±12.0*,†	<0.001
CMR characteristics				
Chamber volumes and mass (indexed to BSA)				
LV EDV, mL/m²	81.1±12.3	70.6±11.7*	67.3±14.4*	<0.001
LV ESV, mL/m²	29.4±6.5	25.3±6.2*	23.2±7.3*,†	<0.001
LV EF, %	63.9±4.5	64.3±5.2	66.0±6.2*,†	0.007
LV mass, g/m²	48.6±12.2	44.3±8.8*	50.5±11.8†	<0.001
LV stroke volume, mL/m²	51.7±7.7	45.2±7.4*	44.1±9.0*	<0.001
LV cardiac output, mL/m² per min	3.25±0.57	3.18±0.63	3.20±0.71	0.65
RV EDV, mL/m²	89.1±14.3	73.0±13.5*	68.5±15.5*,†	<0.001
RV ESV, mL/m²	38.2±8.9	29.4±7.9*	26.8±8.5*,†	<0.001
RV EF, %	57.4±5.0	60.1±6.1*	61.2±6.1*	<0.001
RV stroke volume, mL/m²	50.9±7.6	43.7±8.0*	41.7±9.2*	<0.001
RV cardiac output, mL/m² per min	3.2±0.6	3.1±0.7	3.0±0.7	0.053
LA volume, mL/m²	35.2±7.1	30.6±8.2*	30.6±9.4*	<0.001
3D-MDA‡				
Circumferential strain amplitude, %	−10.9±1.7	−11.7±1.9*	−11.9±2.0*	<0.001
Longitudinal strain amplitude, %	−11.2±1.7	−11.8±1.9*	−12.0±2.1*	0.002
Radial strain amplitude, %	58.2±20.6	70.0±25.7*	69.9±26.2*	<0.001
Minimum principal strain amplitude, %	−26.1±2.8	−28.2±2.6*	−28.4±3.3*	<0.001
Maximum principal strain amplitude (%)	83.2 (67.0–92.8)	98.7 (81.5–119.0)*	99.5 (79.6–134.4)*	<0.001
Systolic circumferential strain rate (1/s)	−0.86±0.16	−0.92±0.14*	−0.97±0.17*,†	<0.001
Systolic longitudinal strain rate (1/s)	−1.01±0.17	−1.12±0.19*	−1.17±0.24*	<0.001
Systolic radial strain rate (1/s)	4.18 (3.44–5.15)	5.07 (4.03–6.39)*	5.36 (3.87–6.65)*	<0.001
Systolic minimum principal strain rate (1/s)	−1.71±0.34	−1.86±0.32*	−1.91±0.43*	<0.001
Systolic maximum principal strain rate (1/s)	5.13 (4.18–6.03)	6.24 (5.01–7.72)*	6.49 (4.99–8.96)*	<0.001
Native T1				
Septum, ms§	1130.0 (1099.0–1157.0)	1164.5 (1142.0–1194.0)*	1174.0 (1142.0–1198.5)*	<0.001
Lateral wall, ms‖	1108.0 (1084.5–1142.5)	1151.0 (1121.0–1189.0)*	1149.0 (1120.0–1176.0)*	<0.001

Values are mean±SD, median (interquartile range), or n (%). 3D-MDA indicates 3-dimensional myocardial deformation analysis; BMI, body mass index; BP, blood pressure; BSA, body surface area; CMR, cardiovascular magnetic resonance; EDV, end-diastolic volume; EF, ejection fraction; ESV, end-systolic volume; LA, left atrium; LV, left ventricle; and RV, right ventricle.

*P<0.05 for post-hoc pairwise comparison of patients with cancer with/without hypertension against healthy volunteers.

†P<0.05 for post-hoc comparison against patients with cancer with no hypertension.

‡Global values; available for 242 patients with non-hypertensive cancer, 115 patients with hypertension and cancer, and 100 healthy volunteers.

§Available for 198 patients with non-hypertensive cancer, 101 patients with hypertensive cancer, and 77 healthy volunteers imaged at 3.0-T.

‖Available for 187 patients with non-hypertensive cancer, 91 patients with hypertensive cancer, and 73 healthy volunteers imaged at 3.0-T.

of geometry-dependent and geometry-independent strain, transmurally and for both endocardial and epicardial layers. Strain amplitudes derived from 3D-based techniques are recognized to have lower absolute values compared with 2D analyses,[23] this believed to be attributable to inherent overestimation of in-plane displacements from 2D analyses from through-plane motion.[32] Versus the reference of CMR tagging, 2D speckle-tracking echocardiography shows positive bias for absolute GLS (+5.5%) whereas 3D speckle-tracking echocardiography shows similar values (−0.5%).[23] Similar bias exists for

Table 7. Baseline Characteristics of Patients With Chemotherapy-Naïve Cancer, Stratified by Diabetes Mellitus, Compared With Healthy Volunteers

Characteristic	Healthy Volunteers (n=102)	Cancer, No DM (n=341)	Cancer, DM (n=40)	P Value
Age, y	43.4±14.5	52.8±13.4*	62.4±10.0*,†	<0.001
BMI, kg/m²	24.9 (22.0, 28.4)	26.3 (23.3, 30.1)*	28.9 (23.2, 36.9)*	0.001
Heart rate, bpm	63.1±9.9	71.2±11.8*	75.5±12.2*	<0.001
Systolic BP, mm Hg	112.8±12.3	116.6±16.1*	122.1±18.9*	0.005
Diastolic BP, mm Hg	66.6±10.0	69.9±11.3*	66.7±9.9	0.010
CMR characteristics				
Chamber volumes and mass (indexed to BSA)				
LV EDV, mL/m²	81.1±12.3	70.1±12.5*	64.1±14.0*,†	<0.001
LV ESV, mL/m²	29.4±6.5	24.8±6.5*	22.7±8.0*	<0.001
LV EF, %	63.9±4.5	64.8±5.4	65.3±6.7	0.19
LV mass, g/m²	48.6±12.2	46.1±10.1	49.5±11.9	0.055
LV stroke volume, mL/m²	51.7±7.7	45.3±7.9*	41.4±7.8*,†	<0.001
LV cardiac output, mL/m² per min	3.3±0.6	3.2±0.7	3.1±0.6	0.34
RV EDV, mL/m²	89.1±14.3	72.4±14.1*	64.4±14.1*,†	<0.001
RV ESV, mL/m²	38.2±8.9	28.8±8.2*	25.7±7.3*,†	<0.001
RV EF, %	57.4±5.0	60.5±6.1*	60.4±6.2*	<0.001
RV stroke volume, mL/m²	50.9±7.6	43.5±8.3*	38.7±8.6*,†	<0.001
RV cardiac output, mL/m² per min	3.2±0.6	3.1±0.7	2.9±0.6*	0.013
LA volume, mL/m²	35.2±7.1	30.7±8.6*	29.4±9.2*	<0.001
3D-MDA‡				
Circumferential strain amplitude, %	−10.9±1.7	−11.7±1.9*	−11.9±2.1*	<0.001
Longitudinal strain amplitude, %	−11.2±1.7	−11.8±1.9*	−12.0±2.2	0.004
Radial strain amplitude, %	58.2±20.6	70.2±26.0*	68.2±24.2	<0.001
Minimum principal strain amplitude, %	−26.1±2.8	−28.3±2.8*	−28.1±3.3*	<0.001
Maximum principal strain amplitude (%)	83.2 (67.0–92.8)	99.3 (82.4–121.8)*	88.2 (76.0–124.5)*	<0.001
Systolic circumferential strain rate (1/s)	−0.86±0.16	−0.93±0.15*	−1.00±0.19*	<0.001
Systolic longitudinal strain rate (1/s)	−1.01±0.17	−1.13±0.20*	−1.18±0.27*	<0.001
Systolic radial strain rate (1/s)	4.18 (3.44–5.15)	5.19 (3.96–6.49)*	4.97 (4.32–6.34)*	<0.001
Systolic minimum principal strain rate (1/s)	−1.71±0.34	−1.87±0.35*	−1.93±0.44*	<0.001
Systolic maximum principal strain rate (1/s)	5.13 (4.18–6.03)	6.36 (4.97–8.01)*	6.35 (5.27–8.27)*	<0.001
Native T1				
Septum, ms§	1130.0 (1099.0–1157.0)	1165.0 (1142.0–1192.0)*	1190.0 (1166.0–1222.0)*,†	<0.001
Lateral wall, ms‖	1108.0 (1084.5–1142.5)	1149.0 (1120.0–1180.5)*	1175.5 (1127.8–1200.0)*	<0.001

Values are mean±SD, median (interquartile range), or n (%). 3D-MDA indicates 3-dimensional myocardial deformation analysis; BMI, body mass index; BP, blood pressure; BSA, body surface area; DM indicates diabetes mellitus; EDV, end-diastolic volume; EF, ejection fraction; ESV, end-systolic volume; LA, left atrium; LV, left ventricle; and RV, right ventricle.

*P<0.05 for post-hoc pairwise comparison of patients with cancer with/without diabetes mellitus against healthy volunteers.

†P<0.05 for post-hoc comparison against patients with cancer with no diabetes mellitus.

‡Global values; available for 322 patients with cancer without diabetes mellitus, 35 patients with cancer and diabetes mellitus, and 100 healthy volunteers.

§Available for 268 patients with cancer and without diabetes mellitus, 31 patients with diabetes mellitus and cancer, and 77 healthy volunteers imaged at 3.0-T.

‖Available for 248 patients with cancer and without diabetes mellitus, 30 patients with diabetes mellitus and cancer, and 73 healthy volunteers imaged at 3.0-T.

2D-feature tracking based strain analysis from CMR cine images, with a bias of +8.4% for GLS.[33] These studies support that 3D strain analyses, as used in the current study, may more accurately reflect true tissue deformation versus 2D techniques.

T1 Mapping

Both septal and lateral wall native T1 values were significantly elevated among patients with cancer compared with HV. This finding is in agreement with a prior study reported by Jordan et al that showed a
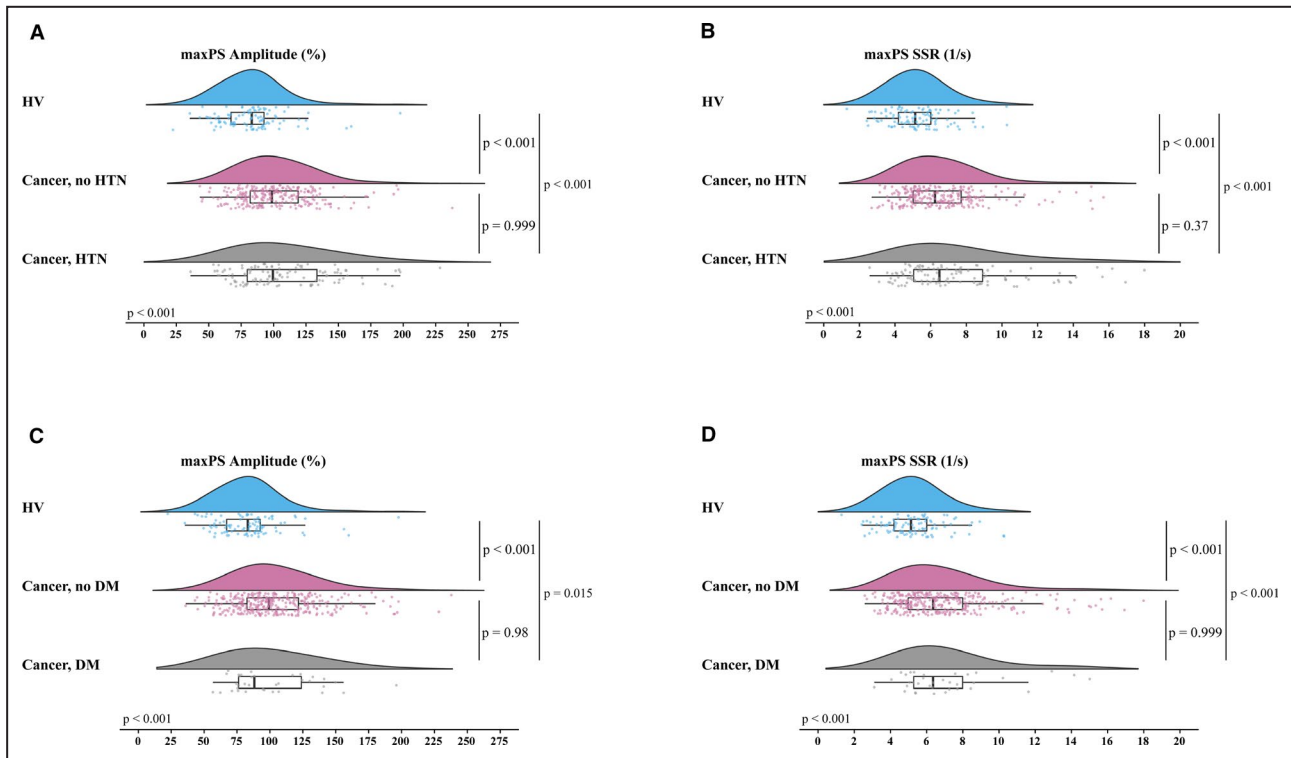
Figure 5. Effect of baseline cardiovascular risk factors on global maximum principal strain amplitude and peak systolic strain rate in patients with cancer vs healthy volunteers.
Strain parameters were similar in patients with cancer with and without hypertension (**A** and **B**) or diabetes mellitus (**C** and **D**) but higher in each cancer subgroup compared with healthy volunteers. DM indicates diabetes mellitus; HV, healthy volunteers; maxPS; maximum principal strain; and SSR, systolic strain rate.

similar degree of T1 elevation in 37 patients with cancer before first chemotherapy exposure.[25] A separate small cohort study of 20 female patients with breast cancer did not observe significant differences; however, it was not designed nor powered to undertake this analysis.[3]

Elevations in native T1, in the absence of concurrent amyloid protein deposition, can be attributed to elevations in tissue water content or collagen-mediated expansion of the interstitium. The latter, while not excluded by our study, appears of lower likelihood for 2 reasons. First, biological plausibility of recently diagnosed cancer (median time from diagnosis 1.2 months) to mediate collagen-based remodelling in this time frame is lower than that of tissue water expansion. Second, collagen-mediated expansion of the interstitium is typically associated with adverse chamber remodelling and reductions in contractile performance, which is opposite to our study findings.

Explaining Influence of Cancer on Cardiovascular Health

The currently described cancer phenotype of reduced chamber volumes (and stroke volume), compensatory tachycardia, elevated myocardial strain, and elevated myocardial T1 can be collectively explained through acknowledgment of known inflammatory pathway activation in active cancer.[29,34–36] Cancer presents a persistent, oncogene-derived cellular stress that establishes a feed-forward loop of inflammatory signaling,[37] this commonly evidenced by elevations in serum inflammatory markers at time of diagnosis.[38] Sustained activation of inflammatory pathways may be anticipated to result in reduction of systemic vascular resistance, reduced chamber volumes, hyper-dynamic contractile state, and elevation in capillary permeability (resulting in increased tissue water). That LV mass was incrementally elevated among patients with breast cancer may represent a unique phenomenon as supported by prior experimental work suggesting a potential role of endothelin-1.[12] Future correlative studies investigating systemic inflammatory and non-inflammatory pathway activation in this population are required to explore such mechanisms.

Relevance to Clinical Practice

A central aspect of cancer care is surveillance of CTRCD following chemotherapy induction. To date, this has been primarily studied in the context of interval changes of LV EF or GLS versus baseline
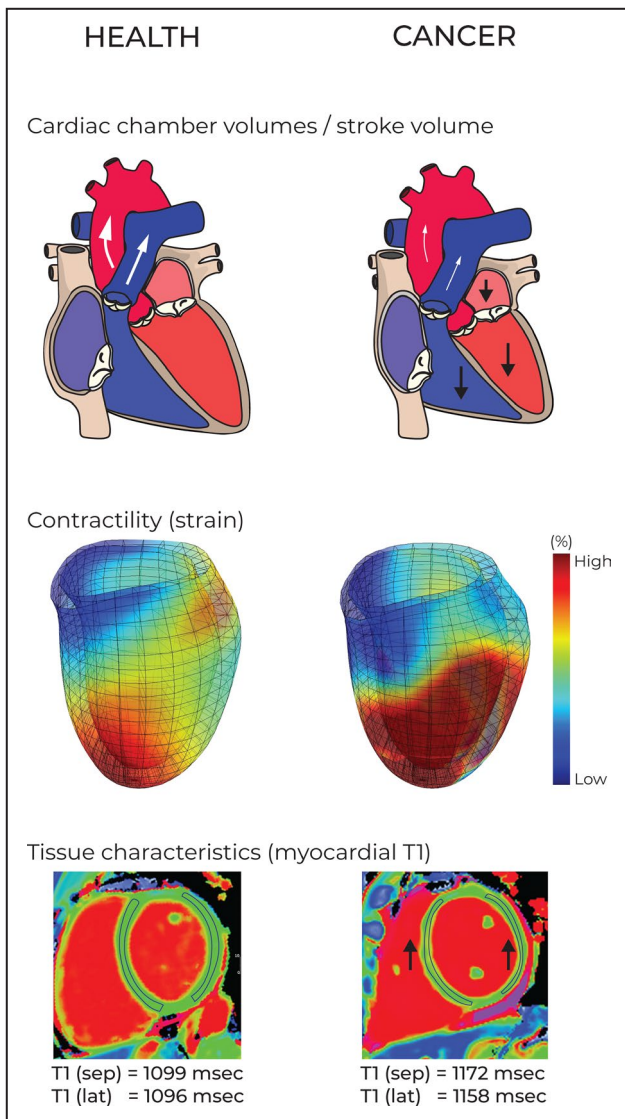
Figure 6. Graphical summary of cancer's effect on the cardiac phenotype.
Compared with a state of health, patients with cancer show reduced cardiac chamber volumes (black arrows) and stroke volumes (white arrows), this compensated for by higher resting heart rate (top panel). Contractility is augmented, with elevation in strain amplitude and systolic strain rate across multiple directions of deformation, as shown by 3-dimensional myocardial deformation analyses in healthy volunteers and a patient with active cancer (maximal principal strain amplitude shown for female healthy volunteers [average values] and an example female patient with cancer; middle panel). This is not reflected through the global measure of left ventricular ejection fraction. Native myocardial T1 is globally elevated (black arrows), as shown by respective short-axis T1 mapping images with both septal (sep) and lateral wall (lat) regions of interest (bottom panel).

phenotype and therefore appear most appropriate in this role. However, the future consideration of strain-based markers, volumetric markers, or serial monitoring of myocardial T1 signal must recognize and carefully weigh these influences.

Whether this observed cancer-mediated state identifies patients at altered risk of subsequent CTRCD or provides value towards the prediction of cancer-related outcomes remains unknown. This will be studied through longitudinal follow-up of the described cohort. However, additional consideration should be given to studying influences of de-novo cancer development in patients with established cardiovascular disease, justified by its demonstrated potential to alter hemodynamic, contractile, and myocardial tissue level characteristics.

Limitations

This study has several important limitations. This was a single-center cohort study; therefore, our results would benefit from external validation in other institutional settings. Despite efforts to recruit healthy volunteers of similar age, a maintained difference versus patients with cancer was observed given greater challenges in identifying qualifying healthy subjects aged >60 years. To address this, we performed multivariable analyses adjusted for age and demonstrated cancer presence remained strongly associated with each CMR parameter. We acknowledge that, while subgroup analysis suggested similar associations between cancer presence and cardiovascular phenotype, the relative number of males represented by this study was modest. Accordingly, future studies aimed at expanding representation for, and evaluating influence in this sex are desirable. Our study was purposely restricted to patients with breast cancer or lymphoma; therefore, our findings are not generalizable to other cancer types. These 2 cancer types were recently identified to be responsible for the majority of heart disease deaths in patients with cancer diagnosed at age <40 years, with breast cancer being 1 of 4 subtypes among those diagnosed at age ≥40 years.[1] While justifying inaugural focus on these cancers, future studies inclusive of other cancer states are of interest and should be pursued. Such studies may assist in elucidating common versus cancer-specific pathways contributing to alterations in cardiovascular phenotype. As intravenous contrast was not administered in this study protocol, late gadolinium enhancement imaging and post-contrast extracellular volume fraction quantification were not performed. Finally, only clinically ordered laboratory testing was available, limiting our capacity to provide incremental comparison to serum-based markers of tissue injury or systemic inflammation.

assessments, these interpreted in the context of healthy cohort reference ranges.[5,16] Fortuitously, these currently recommended global markers of contractile health (LV EF and GLS) showed least sensitivity towards our observed differences in baseline

CONCLUSIONS

Patients with recently diagnosed breast cancer or lymphoma demonstrate a unique cardiovascular phenotype consisting of reduced chamber volumes, elevated strain amplitude and SSR, and elevated myocardial T1. These findings, independent of age, sex, and cardiovascular risk factors, support a meaningful influence of active cancer on the cardiovascular system. Future research is warranted to identify underlying pathophysiologic mechanisms and explore their relevance to clinical outcomes in this population.

ARTICLE INFORMATION

Affiliations

From the Stephenson Cardiac Imaging Centre, Libin Cardiovascular Institute of Alberta, University of Calgary, Alberta, Canada (D.L., A.S., S.D., R.H., Y.M., D.G.G., Z.S., P.F., J.F., S.R., R.S., C.P.L., A.G.H., L.K., J.A.W.); Department of Cardiovascular Medicine, Cairo University, Cairo, Egypt (D.L.); Department of Diagnostic Imaging, Cumming School of Medicine (C.P.L., J.A.W.)and Department of Cardiac Sciences, Cumming School of Medicine (A.G.H., B.C., J.L., J.A.W.), University of Calgary, Alberta, Canada; Department of Medicine, University of Alberta, Edmonton, Alberta, Canada (D.I.P., G.Y.O.); Mazankowski Alberta Heart Institute, University of Alberta, Edmonton, Alberta, Canada (D.I.P., G.Y.O.); Department of Oncology, University of Alberta, Edmonton, Alberta, Canada (E.P.); Departments of Medicine and Oncology, Cumming School of Medicine (W.Y.C.) and Department of Community Health Sciences, Cumming School of MedicineDepartment of Community Health Sciences, Cumming School of Medicine, University of Calgary, Alberta, Canada (J.L.)

Sources of Funding

Disclosures

Supplementary Material

Tables S1–S4

REFERENCES

1. Stoltzfus KC, Zhang Y, Sturgeon K, Sinoway LI, Trifiletti DM, Chinchilli VM, Zaorsky NG. Fatal heart disease among cancer patients. *Nat Commun*. 2020;11:2011. DOI: 10.1038/s41467-020-15639-5.

2. Jordan JH, Castellino SM, Meléndez GC, Klepin HD, Ellis LR, Lamar Z, Vasu S, Kitzman DW, Ntim WO, Brubaker PH, et al. Left ventricular mass change after anthracycline chemotherapy. *Circ Hear Fail*. 2018;11:1–10. DOI: 10.1161/CIRCHEARTFAILURE.117.004560.

3. Altaha MA, Nolan M, Marwick TH, Somerset E, Houbois C, Amir E, Yip P, Connelly KA, Michalowska M, Sussman MS, et al. Can quantitative CMR tissue characterization adequately identify cardiotoxicity during chemotherapy? *JACC Cardiovasc Imaging*. 2020;13:951–962. DOI: 10.1016/j.jcmg.2019.10.016.

4. Negishi T, Thavendiranathan P, Negishi K, Marwick TH, Aakhus S, Murbræch K, Massey R, Bansal M, Fukuda N, Hristova K, et al. Rationale and design of the strain surveillance of chemotherapy for improving cardiovascular outcomes. *JACC Cardiovasc Imaging*. 2018;11:1098–1105. DOI: 10.1016/j.jcmg.2018.03.019.

5. Plana JC, Thavendiranathan P, Bucciarelli-Ducci C, Lancellotti P. Multimodality imaging in the assessment of cardiovascular toxicity in the cancer patient. *JACC Cardiovasc Imaging*. 2018;11:1173–1186. DOI: 10.1016/j.jcmg.2018.06.003.

6. Banke A, Schou M, Videbaek L, Møller JE, Torp-Pedersen C, Gustafsson F, Dahl JS, Køber L, Hildebrandt PR, Gislason GH. Incidence of cancer in patients with chronic heart failure: a long-term follow-up study. *Eur J Heart Fail*. 2016;18:260–266. DOI: 10.1002/ejhf.472.

7. Hasin T, Gerber Y, Weston SA, Jiang R, Killian JM, Manemann SM, Cerhan JR, Roger VL. Heart failure after myocardial infarction is associated with increased risk of cancer. *J Am Coll Cardiol*. 2016;68:265–271. DOI: 10.1016/j.jacc.2016.04.053.

8. Hasin T, Gerber Y, McNallan SM, Weston SA, Kushwaha SS, Nelson TJ, Cerhan JR, Roger VL. Patients with heart failure have an increased risk of incident cancer. *J Am Coll Cardiol*. 2013;62:881–886. DOI: 10.1016/j.jacc.2013.04.088.

9. Sakamoto M, Hasegawa T, Asakura M, Kanzaki H, Takahama H, Amaki M, Mochizuki N, Anzai T, Hamasaki T, Kitakaze M. Does the pathophysiology of heart failure prime the incidence of cancer? *Hypertens Res*. 2017;40:831–836. DOI: 10.1038/hr.2017.45.

10. Bertero E, Canepa M, Maack C, Ameri P. Linking heart failure to cancer. *Circulation*. 2018;138:735–742. DOI: 10.1161/CIRCULATIONAHA.118.033603.

11. Koelwyn GJ, Newman AAC, Afonso MS, van Solingen C, Corr EM, Brown EJ, Albers KB, Yamaguchi N, Narke D, Schlegel M, et al. Myocardial infarction accelerates breast cancer via innate immune reprogramming. *Nat Med*. 2020;26:1452–1458. DOI: 10.1038/s41591-020-0964-7.

12. Maayah ZH, Takahara S, Alam AS, Ferdaoussi M, Sutendra G, El-Kadi AOS, Mackey JR, Pituskin E, Paterson DI, Dyck JRB. Breast cancer diagnosis is associated with relative left ventricular hypertrophy and elevated endothelin-1 signaling. *BMC Cancer*. 2020;20:751. DOI: 10.1186/s12885-020-07217-1.

13. Tian M, Nishijima Y, Asp ML, Stout MB, Reiser PJ, Belury MA. Cardiac alterations in cancer-induced cachexia in mice. *Int J Oncol*. 2010;37:347–353. DOI: 10.3892/ijo_00000683.

14. Mühlfeld C, Das SK, Heinzel FR, Schmidt A, Post H, Schauer S, Papadakis T, Kummer W, Hoefler G. Cancer induces cardiomyocyte remodeling and hypoinnervation in the left ventricle of the mouse heart. *PLoS One*. 2011;6:e20424. DOI: 10.1371/journal.pone.0020424.

15. Seidman A, Hudis C, Pierri MK, Shak S, Paton V, Ashby M, Murphy M, Stewart SJ, Keefe D. Cardiac dysfunction in the trastuzumab clinical trials experience. *J Clin Oncol*. 2002;20:1215–1221. DOI: 10.1200/JCO.2002.20.5.1215.

16. Plana JC, Galderisi M, Barac A, Ewer MS, Ky B, Scherrer-Crosbie M, Ganame J, Sebag IA, Agler DA, Badano LP, et al. Expert consensus for multimodality imaging evaluation of adult patients during and after cancer therapy: a report from the American Society of Echocardiography and the European Association of Cardiovascular Imaging. *J Am Soc Echocardiogr*. 2014;27:911–939. DOI: 10.1016/j.echo.2014.07.012.

17. Piechnik SK, Ferreira VM, Dall'Armellina E, Cochlin LE, Greiser A, Neubauer S, Robson MD. Shortened Modified Look-Locker Inversion recovery (ShMOLLI) for clinical myocardial T1-mapping at 1.5 and 3 T within a 9 heartbeat breathhold. *J Cardiovasc Magn Reson*. 2010;12:69. DOI: 10.1186/1532-429X-12-69.

18. Schulz-Menger J, Bluemke DA, Bremerich J, Flamm SD, Fogel MA, Friedrich MG, Kim RJ, von Knobelsdorff-Brenkenhoff F, Kramer CM, Pennell DJ, et al. Standardized image interpretation and post processing in cardiovascular magnetic resonance: Society for Cardiovascular Magnetic Resonance (SCMR) Board of Trustees Task Force on Standardized Post Processing. *J Cardiovasc Magn Reson*. 2013;15:35. DOI: 10.1186/1532-429X-15-35.

19. Satriano A, Heydari B, Narous M, Exner DV, Mikami Y, Attwood MM, Tyberg JV, Lydell CP, Howarth AG, Fine NM, et al. Clinical feasibility and validation of 3D principal strain analysis from cine MRI: comparison to 2D strain by MRI and 3D speckle tracking echocardiography. *Int J Cardiovasc Imaging*. 2017;33:1979–1992. DOI: 10.1007/s10554-017-1199-7.

20. Satriano A, Heydari B, Guron N, Fenwick K, Cheung M, Mikami Y, Merchant N, Lydell CP, Howarth AG, Fine NM, et al. 3-Dimensional regional and global strain abnormalities in hypertrophic cardiomyopathy. *Int J Cardiovasc Imaging*. 2019;35:1913–1924. DOI: 10.1007/s10554-019-01631-8.

21. Cerqueira MD, Weissman NJ, Dilsizian V, Jacobs AK, Kaul S, Laskey WK, Pennell DJ, Rumberger JA, Ryan T, Verani MS. Standardized myocardial segmentation and nomenclature for tomographic imaging of the heart. *Circulation*. 2002;105:539–542. DOI: 10.1161/hc0402.102975.

22. Pedrizzetti G, Sengupta S, Caracciolo G, Park CS, Amaki M, Goliasch G, Narula J, Sengupta PP. Three-dimensional principal strain analysis for characterizing subclinical changes in left ventricular function. *J Am Soc Echocardiogr*. 2014;27:1041–1050.e1. DOI: 10.1016/j.echo.2014.05.014.

23. Amzulescu MS, Langet H, Saloux E, Manrique A, Slimani A, Allain P, Roy C, de Meester C, Pasquet A, Somphone O, et al. Improvements of myocardial deformation assessment by three-dimensional speckle-tracking versus two-dimensional speckle-tracking revealed by cardiac magnetic resonance tagging. *J Am Soc Echocardiogr*. 2018;31:1021–1033.e1. DOI: 10.1016/j.echo.2018.04.009.

24. Murphy KT. The pathogenesis and treatment of cardiac atrophy in cancer cachexia. *Am J Physiol Heart Circ Physiol*. 2016;310:H466–H477. DOI: 10.1152/ajpheart.00720.2015.

25. Jordan JH, Vasu S, Morgan TM, D'Agostino RB, Meléndez GC, Hamilton CA, Arai AE, Liu S, Liu C-Y, Lima JAC, et al. Anthracycline-associated T1 mapping characteristics are elevated independent of the presence of cardiovascular comorbidities in cancer Survivors. *Circ Cardiovasc Imaging*. 2016;9:1–19. DOI: 10.1161/CIRCIMAGING.115.004325.

26. Tadic M, Genger M, Baudisch A, Kelle S, Cuspidi C, Belyavskiy E, Burkhardt F, Venneri L, Attanasio P, Pieske B. Left ventricular strain in chemotherapy-naive and radiotherapy-naive patients with cancer. *Can J Cardiol*. 2018;34:281–287. DOI: 10.1016/j.cjca.2017.11.018.

27. Tadic M, Baudisch A, Haßfeld S, Heinzel F, Cuspidi C, Burkhardt F, Escher F, Attanasio P, Pieske B, Genger M. Right ventricular function and mechanics in chemotherapy- and radiotherapy-naïve cancer patients. *Int J Cardiovasc Imaging*. 2018;34:1581–1587. DOI: 10.1007/s10554-018-1379-0.

28. Assuncao BMBL, Handschumacher MD, Brunner AM, Yucel E, Bartko PE, Cheng K-H, Campos O, Fathi AT, Tan TC, Scherrer-Crosbie M. Acute leukemia is associated with cardiac alterations before chemotherapy. *J Am Soc Echocardiogr*. 2017;30:1111–1118. DOI: 10.1016/j.echo.2017.07.016.

29. Cramer L, Hildebrandt B, Kung T, Wichmann K, Springer J, Doehner W, Sandek A, Valentova M, Stojakovic T, Scharnagl H, et al. Cardiovascular function and predictors of exercise capacity in patients with colorectal cancer. *J Am Coll Cardiol*. 2014;64:1310–1319. DOI: 10.1016/j.jacc.2014.07.948.

30. Mavinkurve-Groothuis AMC, Marcus KA, Pourier M, Loonen J, Feuth T, Hoogerbrugge PM, de Korte CL, Kapusta L. Myocardial 2D strain echocardiography and cardiac biomarkers in children during and shortly after anthracycline therapy for acute lymphoblastic leukaemia (ALL): a prospective study. *Eur Heart J Cardiovasc Imaging*. 2013;14:562–569. DOI: 10.1093/ehjci/jes217.

31. Akam-Venkata J, Kadiu G, Galas J, Aggarwal S. Pediatric malignancies: Is the prechemotherapy left ventricular function normal? *Echocardiography*. 2019;36:1727–1735. DOI: 10.1111/echo.14461.

32. Pedrizzetti G, Claus P, Kilner PJ, Nagel E. Principles of cardiovascular magnetic resonance feature tracking and echocardiographic speckle tracking for informed clinical use. *J Cardiovasc Magn Reson*. 2016;18:51. DOI: 10.1186/s12968-016-0269-7.

33. Bucius P, Erley J, Tanacli R, Zieschang V, Giusca S, Korosoglou G, Steen H, Stehning C, Pieske B, Pieske-Kraigher E, et al. Comparison of feature tracking, fast-SENC, and myocardial tagging for global and segmental left ventricular strain. *ESC Hear Fail*. 2020;7:523–532. DOI: 10.1002/ehf2.12576.

34. Łukaszewicz-Zając M, Mroczko B, Gryko M, Kędra B, Szmitkowski M. Comparison between clinical significance of serum proinflammatory proteins (IL-6 and CRP) and classic tumor markers (CEA and CA 19–9) in gastric cancer. *Clin Exp Med*. 2011;11:89–96. DOI: 10.1007/s10238-010-0114-5.

35. Weinstein PS, Skinner M, Sipe JD, Lokich JJ, Zamcheck N, Cohen AS. Acute-phase proteins or tumour markers: the role of SAA, SAP, CRP and CEA as indicators of metastasis in a broad spectrum of neoplastic diseases. *Scand J Immunol*. 1984;19:193–198. DOI: 10.1111/j.1365-3083.1984.tb00919.x.

36. Ausoni S, Calamelli S, Saccà S, Azzarello G. How progressive cancer endangers the heart: an intriguing and underestimated problem. *Cancer Metastasis Rev*. 2020;39:535–552. DOI: 10.1007/s10555-020-09869-8.

37. Greten FR, Grivennikov SI. Inflammation and cancer: triggers, mechanisms, and consequences. *Immunity*. 2019;51:27–41. DOI: 10.1016/j.immuni.2019.06.025.

38. Asegaonkar SB, Asegaonkar BN, Takalkar UV, Advani S, Thorat AP. C-reactive protein and breast cancer: new insights from old molecule. *Int J Breast Cancer*. 2015;2015:1–6. DOI: 10.1155/2015/145647.

SUPPLEMENTAL MATERIAL

Table S1. Baseline cardiac chamber volumes and LV mass indexed to height in chemotherapy-naïve cancer patients compared to healthy volunteers, stratified by sex

Characteristic	Healthy volunteers	Cancer patients	p-value
Females	N = 55	N = 300	
LV EDV, mL/m	81.6 ± 13.3	75.2 ± 15.1	**0.002**
LV ESV, mL/m	28.8 ± 6.7	26.4 ± 7.6	**0.021**
LV mass, g/m	43.3 ± 7.4	49.1 ± 11.7	**<0.001**
LV stroke volume, mL/m	52.8 ± 9.0	48.7 ± 9.5	**0.003**
LV cardiac output, mL/m/min	3.4 ± 0.8	3.5 ± 0.8	0.73
RV EDV, mL/m	86.9 ± 13.5	76.5 ± 15.7	**<0.001**
RV ESV, mL/m	35.8 ± 8.1	30.1 ± 8.4	**<0.001**
RV stroke volume, mL/m	51.1 ± 7.7	46.4 ± 9.6	**<0.001**
RV cardiac output, mL/m/min	3.3 ± 0.7	3.3 ± 0.8	0.63
LA volume, mL/m	36.5 ± 6.9	33.5 ± 10.0	**0.009**
Males	N = 47	N = 81	
LV EDV, mL/m	96.5 ± 12.7	86.9 ± 17.9	**<0.001**
LV ESV, mL/m	35.9 ± 6.6	31.5 ± 8.7	**0.002**
LV mass, g/m	65.2 ± 14.3	63.9 ± 17.3	0.65
LV stroke volume, mL/m	60.5 ± 7.8	55.4 ± 11.7	**0.003**
LV cardiac output, mL/m/min	3.7 ± 0.7	4.0 ± 0.9	0.051
RV EDV, mL/m	109.1 ± 13.9	92.9 ± 21.8	**<0.001**
RV ESV, mL/m	48.6 ± 8.8	38.7 ± 12.5	**<0.001**
RV stroke volume, mL/m	60.5 ± 8.0	54.2 ± 11.8	**<0.001**
RV cardiac output, mL/m/min	3.7 ± 0.7	3.9 ± 0.9	0.18
LA volume, mL/m	40.5 ± 9.2	37.2 ± 13.0	0.10

Values are mean ± SD, median (IQR), or n (%). LV indicates left ventricle; EDV, end-diastolic volume; ESV, end-systolic volume; RV, right ventricle; and LA, left atrium.

Table S2. Baseline global layer-specific (subendocardial and subepicardial) strain by 3D-MDA in chemotherapy-naïve cancer patients compared to healthy volunteers, stratified by sex

Characteristic	Healthy volunteers	Cancer patients	p-value
Females	**N = 55**	**N = 285**	
Subendocardial circumferential strain amplitude (%)	-14.6 ± 2.3	-15.4 ± 2.3	**0.040**
Subepicardial circumferential strain amplitude (%)	-8.0 ± 1.4	-8.6 ± 1.7	**0.011**
Subendocardial longitudinal strain amplitude (%)	-14.3 ± 2.2	-14.8 ± 2.3	0.11
Subepicardial longitudinal strain amplitude (%)	-8.8 ± 1.5	-8.7 ± 1.9	0.56
Subendocardial minimum principal strain amplitude (%)	-28.7 ± 2.3	-30.4 ± 2.7	**<0.001**
Subepicardial minimum principal strain amplitude (%)	-25.1 ± 2.3	-26.4 ± 2.5	**<0.001**
Subendocardial circumferential systolic strain rate (1/s)	-1.10 ± 0.19	-1.16 ± 0.19	**0.013**
Subepicardial circumferential systolic strain rate (1/s)	-0.71 ± 0.13	-0.74 ± 0.12	0.13
Subendocardial longitudinal systolic strain rate (1/s)	-1.27 ± 0.18	-1.42 ± 0.28	**<0.001**
Subepicardial longitudinal systolic strain rate (1/s)	-0.87 ± 0.15	-0.91 ± 0.16	0.059
Subendocardial minimum principal systolic strain rate (1/s)	-1.83 ± 0.37	-1.99 ± 0.39	**0.005**
Subepicardial minimum principal systolic strain rate (1/s)	-1.69 ± 0.35	-1.76 ± 0.33	0.18
Males	**N = 45**	**N = 72**	
Subendocardial circumferential strain amplitude (%)	-14.6 ± 2.4	-15.3 ± 3.2	0.18
Subepicardial circumferential strain amplitude (%)	-7.5 ± 1.3	-8.6 ± 2.1	**<0.001**
Subendocardial longitudinal strain amplitude (%)	-13.6 ± 2.0	-14.6 ± 3.0	**0.028**
Subepicardial longitudinal strain amplitude (%)	-8.0 ± 1.3	-8.8 ± 2.1	**0.016**
Subendocardial minimum principal strain amplitude (%)	-27.1 ± 3.1	-29.1 ± 3.2	**<0.001**
Subepicardial minimum principal strain amplitude (%)	-22.5 ± 2.6	-24.3 ± 3.3	**0.001**
Subendocardial circumferential systolic strain rate (1/s)	-1.08 ± 0.21	-1.24 ± 0.22	**<0.001**
Subepicardial circumferential systolic strain rate (1/s)	-0.65 ± 0.13	-0.78 ± 0.15	**<0.001**

Characteristic	Healthy volunteers	Cancer patients	p-value
Subendocardial longitudinal systolic strain rate (1/s)	-1.23 ± 0.23	-1.47 ± 0.29	**<0.001**
Subepicardial longitudinal systolic strain rate (1/s)	-0.79 ± 0.14	-0.95 ± 0.18	**<0.001**
Subendocardial minimum principal systolic strain rate (1/s)	-1.75 ± 0.37	-2.02 ± 0.44	**<0.001**
Subepicardial minimum principal systolic strain rate (1/s)	-1.58 ± 0.32	-1.78 ± 0.41	**0.004**

Values are mean ± SD, median (IQR), or n (%)

Table S3. Baseline characteristics of female chemotherapy-naïve cancer patients, stratified by type of cancer, compared to healthy volunteers

Characteristic	Healthy volunteers (n = 55)	Breast cancer (n = 242)	Lymphoma (n = 58)	p-value
Age, years	41.9 ± 13.8	$51.3 \pm 10.9^*$	$57.5 \pm 17.8^{*\dagger}$	**<0.001**
BMI, kg/m^2	24.1 (21.0, 27.7)	26.6 (23.0, 31.3)*	25.4 (22.6, 29.0)	**0.001**
Heart rate, bpm	64.7 ± 10.3	$71.2 \pm 11.7^*$	$72.4 \pm 11.6^*$	**<0.001**
Systolic BP, mmHg	110.9 ± 12.5	$116.0 \pm 15.1^*$	$118.4 \pm 16.6^*$	**0.012**
Diastolic BP, mmHg	65.8 ± 9.2	69.1 ± 11.2	68.5 ± 11.3	0.07
CMR characteristics				
Chamber volumes and mass (indexed to BSA)				
LV EDV, mL/m^2	77.9 ± 12.0	$68.4 \pm 11.9^*$	$66.4 \pm 11.1^*$	**<0.001**
LV ESV, mL/m^2	27.6 ± 6.4	$24.1 \pm 6.5^*$	$23.3 \pm 5.9^*$	**0.001**
LV EF, %	64.8 ± 5.0	65.1 ± 5.6	65.1 ± 5.2	0.90
LV mass, g/m^2	41.3 ± 6.6	$44.2 \pm 8.5^*$	44.4 ± 8.2	**0.020**
LV stroke volume, mL/m^2	50.3 ± 7.8	$44.4 \pm 7.4^*$	$43.1 \pm 7.2^*$	**<0.001**
LV cardiac output, mL/m^2/min	3.3 ± 0.6	3.1 ± 0.6	3.1 ± 0.6	0.35
RV EDV, mL/m^2	83.1 ± 12.7	$69.5 \pm 12.4^*$	$68.6 \pm 13.3^*$	**<0.001**
RV ESV, mL/m^2	34.3 ± 7.8	$27.2 \pm 7.2^*$	$27.3 \pm 7.5^*$	**<0.001**
RV EF, %	59.0 ± 5.0	$61.0 \pm 6.2^*$	60.5 ± 5.8	**0.038**
RV stroke volume, mL/m^2	48.8 ± 7.0	$42.2 \pm 7.8^*$	$41.3 \pm 7.8^*$	**<0.001**
RV cardiac output, mL/m^2/min	3.2 ± 0.6	3.0 ± 0.6	2.9 ± 0.7	0.067
LA volume, mL/m^2	34.8 ± 6.0	$30.8 \pm 7.8^*$	$27.9 \pm 8.8^*$	**<0.001**
3D-MDA (transmural values)[‡]				
Circumferential strain amplitude (%)	-11.1 ± 1.8	$-11.8 \pm 1.8^*$	-11.7 ± 1.7	**0.028**
Longitudinal strain amplitude (%)	-11.6 ± 1.7	-11.9 ± 1.9	-11.9 ± 1.7	0.55
Radial strain amplitude (%)	64.3 ± 19.1	71.3 ± 25.8	73.4 ± 28.3	**0.050**

Characteristic	Healthy volunteers (n = 55)	Breast cancer (n = 242)	Lymphoma (n = 58)	p-value
Minimum principal strain amplitude (%)	-27.0 ± 2.3	-28.6 ± 2.6[*]	-28.8 ± 2.4[*]	**<0.001**
Maximum principal strain amplitude (%)	88.8 (79.3, 95.8)	101.3 (83.7, 124.2)[*]	105.7 (92.2, 131.1)[*]	**<0.001**
Systolic circumferential strain rate (1/s)	-0.88 ± 0.15	-0.92 ± 0.15	-0.96 ± 0.13[*]	**0.019**
Systolic longitudinal strain rate (1/s)	-1.05 ± 0.16	-1.12 ± 0.21[*]	-1.18 ± 0.19[*]	**0.001**
Systolic radial strain rate (1/s)	4.38 (3.90, 5.21)	5.11 (4.08, 6.44)[*]	5.67 (3.87, 6.95)[*]	**0.008**
Systolic minimum principal strain rate (1/s)	-1.75 ± 0.35	-1.85 ± 0.34	-1.94 ± 0.34[*]	**0.016**
Systolic maximum principal strain rate (1/s)	5.50 (4.67, 6.25)	6.30 (5.13, 7.83)[*]	6.96 (5.31, 8.51)[*]	**<0.001**
Native T1				
Septum, ms[§]	1143.5 (1121.3, 1161.0)	1167.0 (1139.5, 1188.0)[*]	1163.0 (1148.0, 1206.0)[*]	**<0.001**
Lateral wall, ms[‖]	1130.0 (1096.3, 1165.8)	1147.0 (1120.0, 1177.8)	1162.0 (1118.0, 1201.0)[*]	**0.031**

Values are mean ± SD, median (IQR), or n (%). BMI indicates body mass index; BP, blood pressure; BSA, body surface area; LV, left ventricle; EDV, end-diastolic volume; ESV, end-systolic volume; EF, ejection fraction; RV, right ventricle; LA, left atrium; and 3D-MDA, three-dimensional myocardial deformation analysis.

[*]p-value < 0.05 for post-hoc pairwise comparison of individual type of cancer against healthy controls

[†]p-value < 0.05 for post-hoc comparison against breast cancer patients

[‡]Global values; available for 233 breast cancer, 52 lymphoma patients and 55 healthy controls

[§]Available for 189 breast cancer, 49 lymphoma patients and 38 healthy controls imaged at 3.0-T

[‖]Available for 180 breast cancer, 45 lymphoma patients and 36 healthy controls imaged at 3.0-T

Table S4 Baseline characteristics of male chemotherapy-naïve lymphoma patients, compared to healthy volunteers

Characteristic	Healthy volunteers (n = 47)	Cancer patients (n = 77)	p-value
Age, years	45.1 ± 15.3	59.3 ± 14.7	**<0.001**
BMI, kg/m^2	26.2 (24.4, 28.9)	26.6 (24.5, 31.1)	0.26
Heart rate, bpm	61.3 ± 9.3	73.2 ± 12.6	**<0.001**
Systolic BP, mmHg	115.2 ± 11.8	120.0 ± 20.2	0.11
Diastolic BP, mmHg	67.7 ± 11.0	71.6 ± 10.8	0.066
CMR characteristics			
Chamber volumes and mass (indexed to BSA)			
LV EDV, mL/m^2	84.9 ± 11.8	74.5 ± 15.0	**<0.001**
LV ESV, mL/m^2	31.6 ± 5.9	27.0 ± 7.5	**<0.001**
LV EF, %	62.9 ± 3.7	64.0 ± 6.0	0.23
LV mass, g/m^2	57.2 ± 11.8	54.2 ± 12.7	0.19
LV stroke volume, mL/m^2	53.3 ± 7.3	47.5 ± 9.8	**<0.001**
LV cardiac output, mL/m^2/min	3.2 ± 0.50	3.5 ± 0.8	0.084
RV EDV, mL/m^2	96.1 ± 12.9	79.3 ± 17.3	**<0.001**
RV ESV, mL/m^2	42.8 ± 7.9	32.9 ± 9.9	**<0.001**
RV EF, %	55.6 ± 4.5	58.8 ± 5.9	**<0.001**
RV stroke volume, mL/m^2	53.3 ± 7.6	46.4 ± 9.9	**<0.001**
RV cardiac output, mL/m^2/min	3.3 ± 0.5	3.4 ± 0.8	0.34
LA volume, mL /m^2	35. 7 ± 8.3	31.9 ± 10.5	**0.028**
3D-MDA (transmural values)[*]			
Circumferential strain amplitude (%)	-10.7 ± 1.7	-11.6 ± 2.4	**0.020**

Characteristic	Healthy volunteers (n = 47)	Cancer patients (n = 77)	p-value
Longitudinal strain amplitude (%)	-10.6 ± 1.4	-11.6 ± 2.3	**0.005**
Radial strain amplitude (%)	50.8 ± 20.1	63.3 ± 23.2	**0.003**
Minimum principal strain amplitude (%)	-24.9 ± 2.9	-26.9 ± 3.3	**<0.001**
Maximum principal strain amplitude (%)	67.5 (57.8, 86.2)	87.1 (70.3, 102.9)	**0.002**
Systolic circumferential strain rate (1/s)	-0.84 ± 0.17	-0.98 ± 0.18	**<0.001**
Systolic longitudinal strain rate (1/s)	-0.97 ± 0.17	-1.16 ± 0.21	**<0.001**
Systolic radial strain rate (1/s)	3.70 (3.04, 4.42)	4.79 (3.85, 6.32)	**<0.001**
Systolic minimum principal strain rate (1/s)	-1.66 ± 0.33	-1.90 ± 0.42	**0.001**
Systolic maximum principal strain rate (1/s)	4.56 (3.51, 5.91)	5.68 (4.72, 7.62)	**<0.001**
Native T1			
Septum, ms[†]	1104.0 (1073.0, 1140.0)	1174.0 (1142.0, 1210.5)	**<0.001**
Lateral wall, ms[‡]	1096.0 (1069.5, 1122.5)	1155.0 (1130.0, 1194.0)	**<0.001**

Values are mean ± SD, median (IQR), or n (%). HV indicates healthy volunteers; BMI, body mass index; BP, blood pressure; BSA, body surface area; LV, left ventricle; EDV, end-diastolic volume; ESV, end-systolic volume; EF, ejection fraction; RV, right ventricle; LA, left atrium; and 3D-MDA, three-dimensional myocardial deformation analysis.

[*]Global values; available for 62 cancer patients and 45 healthy controls

[†]Available for 57 cancer patients and 39 healthy controls

[‡]Available for 49 cancer patients and 37 healthy controls